

Journal Pre-proof

In silico, in vitro and in vivo studies indicate resveratrol analogue as a potential alternative for neuroinflammatory disorders

Pollyana Mendonça de Assis, Amanda Fávero, Jaíne Ferrareis Menegasso, Raissa Soares Meinel, Gabriel Macedo Marion, Vinicius Schmitz Pereira Nunes, Priscila Vanessa Zabala Capriles Goliatt, Adilson David da Silva, Rafael Cypriano Dutra, Nádia Rezende Barbosa Raposo



PII: S0024-3205(20)30286-1

DOI: <https://doi.org/10.1016/j.lfs.2020.117538>

Reference: LFS 117538

To appear in: *Life Sciences*

Received date: 16 November 2019

Revised date: 3 March 2020

Accepted date: 8 March 2020

Please cite this article as: P.M. de Assis, A. Fávero, J.F. Menegasso, et al., In silico, in vitro and in vivo studies indicate resveratrol analogue as a potential alternative for neuroinflammatory disorders, *Life Sciences*(2020), <https://doi.org/10.1016/j.lfs.2020.117538>

This is a PDF file of an article that has undergone enhancements after acceptance, such as the addition of a cover page and metadata, and formatting for readability, but it is not yet the definitive version of record. This version will undergo additional copyediting, typesetting and review before it is published in its final form, but we are providing this version to give early visibility of the article. Please note that, during the production process, errors may be discovered which could affect the content, and all legal disclaimers that apply to the journal pertain.

In silico, in vitro and in vivo studies indicate resveratrol analogue as a potential alternative for neuroinflammatory disorders

Pollyana Mendonça de Assis^a, Amanda Fávero^a, Jaíne Ferrareis Menegasso^b, Raissa Soares Meinel^c, Gabriel Macedo Marion^d, Vinicius Schmitz Pereira Nunes^d, Priscila Vanessa Zabala Capriles Goliatt^d, Adilson David da Silva^c, Rafael Cypriano Dutra^b, Nádia Rezende Barbosa Raposo^a

^a NUPICS, Faculty of Pharmacy, Federal University of Juiz de Fora, Juiz de Fora, MG, Brazil

^b Laboratory of Autoimmunity and Immunopharmacology (LAIF), Federal University of Santa Catarina, 88906-072, Araranguá, Santa Catarina, Brazil.

^c Chemistry Department, Federal University of Juiz de Fora, Juiz de Fora, MG, Brazil

^d Graduate Program in Computational Modeling, Department of Computer Science, Federal University of Juiz de Fora, Juiz de Fora, MG, Brazil

*Corresponding author at:

Rua José Lourenço Kelmer, s/n, Campus Universitário, 36036-900, Juiz de Fora, MG, Brazil. Tel/Fax: +55 32 21023809.

E-mail address: nadiacritt@gmail.com

Abstract

Inflammaging is known as an imbalance between pro-inflammatory and anti-inflammatory immune mechanisms, being related to the onset of neurological disorders, such as major depression and Alzheimer's disease. Considering the known disadvantages regarding the FDA approved drug to manage such illnesses, resveratrol emerges as a natural drug candidate, despite its low bioavailability. In this study, resveratrol analogues were evaluated for their capacity of inhibiting acetylcholinesterase *in silico*, *in vitro*, and *in vivo*. Molecular docking simulations pointed out RSVA1 and RSVA6 as potent inhibitors, even more than resveratrol. Ellman's assay demonstrated RSVA6 as capable of inhibiting 92.4% of the enzyme activity. Further, male Swiss mice were pretreated with RSVA6 (100 mg kg⁻¹) 60 min before receiving scopolamine (1 mg kg⁻¹). The Novel Recognition Object (NOR), Object Location (OLT), and Buried Pellet tests (BPL) demonstrated an RSVA6 neuroprotective effect. In the second round of tests, mice received a single intraperitoneal injection of lipopolysaccharide (0.5 mg kg⁻¹) 24 h before treatment with RSVA6 (1, 10, and 100 mg kg⁻¹). The Open Field (OFT), Tail Suspension (TST), and Splash tests (ST) were evaluated. LPS had no significant effect on the crossing and rearing number, indicating an association between the immobility time and anhedonia observed in the TST and ST, respectively, with depressive-like behavior. RSVA6 significantly reduced the depressive-like behavior triggered by LPS in the TST and ST. Altogether, our data suggest RSVA6 as a potential drug candidate for the treatment of neuroinflammatory conditions.

Keywords: resveratrol, acetylcholinesterase, scopolamine, lipopolysaccharide, homology modeling, protein-ligand docking.

1. INTRODUCTION

Inflammaging is known as a multifactorial and age-related imbalance between pro-inflammatory and anti-inflammatory immune mechanisms resulted from lifelong processes of stressor exposures that promote a progressive increase of the inflammatory status [1-3]. In the brain, aging may be responsible for morphological and functional changes in neurons and glial cells. Since microglia are the major immune mediators of the central nervous system (CNS) secreting inflammatory cytokines and reactive oxygen species (ROS), any alteration in activation and regulation of these cells can lead to a brain chronic inflammatory state [4]. When in this state, the activated microglia over-produce different pro-inflammatory cytokines (e.g., TNF, IL-1 β , and IL-6) [5] consecutively exposing neurons to various inflammatory mediators that can stimulate neuronal cell injury or death [6]. Recently, neuron loss has been associated with the release of high mobility group box-1 (HMGB1) protein in the extracellular *milieu*. This protein acts as a damage-associated molecular pattern (DAMP) capable of activating inflammatory processes through receptor for advanced glycation end products (RAGE) and toll-like receptor 4 (TLR4) linkage, playing an important role in inflammation [7]. Altogether, immunescence associated with inflammaging plus up-regulation of systemic inflammation may remodulate the neural-immune cells and lead to a chronic low-grade inflammation in the brain, also known as neuroinflammation [8].

Some evidence has been indicating a relationship between the acceleration of the inflammaging process and the onset and development of age-related chronic neuroinflammatory and neurodegenerative disorders [9,10], including Parkinson disease (PD), amyotrophic lateral sclerosis, Alzheimer disease (AD) [11], and depression [5]. According to the “neuroinflammatory hypothesis” of AD, A β plaques and intracellular tangles can act as pro-inflammatory agents, stimulating the proliferation and activation of astrocytes and microglia. Once activated, those cells produce cytokines responsible for triggering signaling cascades that lead to brain dysfunction and cognitive deterioration, with further neuronal death [12]. The cholinergic dysfunction, one of the consequences of the loss of cholinergic innervation, has been attributed as the main cause of early AD symptoms [13]. Not by chance, targeting the cholinergic system is still an essential approach for developing new strategies for AD patients [14]. Major depressive disorder (MDD) may be a comorbid condition found in AD patients, and during the past years, inflammation has been considered a common link between both of those illnesses [15].

However, the current FDA approved drugs for managing neurological and neuropsychiatric disorders have considerable disadvantages. For AD, for example, at least half of the patients are unresponsive to the acetylcholinesterase inhibitors (iAChE) (donepezil, rivastigmine, galantamine) [16]. Likewise, the available antidepressants (i.e., selective serotonin reuptake inhibitors, selective noradrenaline reuptake inhibitors, monoamine oxidase inhibitors, and tricycles) are associated with many side effects and a variety of clinical responses [17,18].

According to Freires and colleagues [19], the use of animal models had been supported scientific experimentation by predicting efficacy, mechanistic, and toxicological insights in drug discovery. Scopolamine, a non-selective muscarinic antagonist, is employed to trigger cognitive impairments related to learning and memory behaviors in animal models [20]. The similarity between the alteration caused by the drug in the CNS and the early symptoms observed in AD made the scopolamine a widely accepted pattern to assess new drugs with potential

cognitive effects [21]. Intraperitoneal injection of lipopolysaccharide (LPS - outer-membrane endotoxin of Gram-negative bacteria) is known to prompt neuroinflammation [22]. The LPS-induced microglia activation through TLR4 triggers an innate immune response leading to the sickness behavior, characterized by apathy, relative inertia, and curling up the body that changes to a depressive-like behavior for up to 24 h later the LPS administration [5,23]. For this reason, LPS-induced systemic inflammation in animal models is commonly used to investigate neurological disorders [24].

Resveratrol (RSV; 3,5,4'-trihydroxystilbene) is a polyphenol commonly found in the barks of purple grapes and red wine. In addition to its widely known and studied antioxidant action, RSV still exhibits anti-inflammatory [25], anticancer [26], cardioprotective [27], and antiprotozoal activities [28,29]. Furthermore, this stilbene has also been reported as improving cognitive and non-cognitive impairments, such as learning, memory, anxiety, and depression [30], as well as demonstrated positive results in AD [31].

Despite the well-described biological activities, RSV low bioavailability is still a limiting factor for its use in pharmacological purposes [28,32,33]. In this sense, the development of RSV analogues may surpass this problem. For this study, a combination of *in silico*, *in vitro*, and *in vivo* studies was applied in a series of RSV analogues showing their potential as iAChE, neuroprotective and antidepressant-like, indicating these compounds as possible candidates for developing new drugs for the treatment of neuroinflammatory disorders.

2. EXPERIMENTAL SECTION

2.1. Materials

All chemicals, organic solvents (ethanol), reagents (aniline and aromatic aldehydes), acetylcholine iodide (AChI), 5,5'-dithiobis-(2-nitrobenzoic acid) (DTNB), physostigmine (Eserin), dimethyl sulfoxide (DMSO), scopolamine and lipopolysaccharides (LPS) were purchased from Sigma-Aldrich Chemical Co., St. Louis, USA.

2.2. Chemistry

A series of resveratrol analogues (RSVA1-8) were synthesized utilizing a classical method of imine formation that consists of the condensation of aniline with several different aromatic aldehydes, using ethanol as solvent at room temperature (Scheme 1). The structure of these compounds was characterized by ^1H and ^{13}C RMN and melting point (Table 1), being in agreement with the literature.

2.3. *In silico* experiments

2.3.1. Molecular modeling

Considering the *in vitro* assays were performed using the commercial AChET obtained from *Electrophorus electricus*, and *in vivo* assays were performed on *Mus musculus*, we modeled the tetrameric conformation of

acetylcholinesterase (AChET) of *E. electricus* (EeAChET), *Mus musculus* (MmAChET) and *Homo sapiens* (HsAChET) to validate the computational studies. The models were then used in molecular docking simulations.

The amino acid sequences of the enzymes were obtained from the UniProt database (UniProt Consortium, 2017): O42275 (EeAChET), P21836 (MmAChET) and P22303 (HsAChE). Each sequence was submitted to the SignalP server for signal peptide identification. Once identified, the sequence was removed from the template and, therefore, not modeled.

Crystallographic structures were searched in the PDB (Protein Data Bank) to find suitable templates for the construction of the EeAChET, MmAChET, and HsAChET models. Several AChE structures (EC 3.1.1.7) fitted the search criteria (high identity and similarity with human AChE), but only two presented tetrameric conformation: 1C2O and 1MAA from *M. musculus*. The 1C2O structure has a 4.5 Å of resolution while 1MAA has 2.9 Å, and both are classified as a non-planar and antiparallel tetramer [34,35]. An important difference between these structures is that chains A and D of 1C2O partially blocking the active site of chains B and D, whereas, in structure 1MAA, such obstruction is not observed showing that the non-planar conformation of the tetramer exhibits significant conformational flexibility [34]. 1MMA structure presents both better resolution and active site accessibility of the four chains than 1C2O. Thus, 1MMA was selected as a template to modeling the EeAChET, MmAChET, and HsAChET tetramers.

In the attempt to understand the active site affinity to acetylcholine (Ach) and other known inhibitors and to complete the three-dimensional (3D) model of the tetrameric structures, other crystallographic structures were selected as template: 1MAA, 4M0E (chain B), 4M0F (chain B), 2HA4 (chain b), and 1VZJ. The values of sequence identity and similarity between HsAChET and templates are 91% / 93% (1MAA), 97% / 97% (4M0E), 97% / 97% (4M0F), 86% / 91 % (2HA4), and 100% / 100% (1VZJ). For MmAChET, the respective values are 97% / 97% (1MAA), 84% / 89% (4M0E), 84% / 89% (4M0F), 95% / 95% (2HA4) and 100% / 100% (1VZJ). And for EeAChET, the respective values are 58% / 70% (1MAA), 57% / 70% (4M0E), 57% / 70% (4M0F), 58% / 70% (2HA4) and 80% / 98% (1VZJ).

The 4M0E and 4M0F structures of *H. sapiens* were selected as templates due to the presence of AChE inhibitors, territre and dihydrotanshinone. The use of 2HA4 of *M. musculus* as a template was justified by the presence of the substrate Ach. The ligands present in the crystallographic structures were kept during the modeling process of EeAChET and HsAChET. The *H. sapiens* crystallographic structure 1VZJ is the only one in the PDB databank that corresponds to a more elongated alpha-helix in the C-terminus region of the AChE. This region is the result of alternative splicing that maintains the exon 6 in the primary structure of the AChE, forming the AChET isoform [36]. Also, part of the 1VZJ structure is a stretch of residues that correspond to the PRAD (Proline-Rich Attachment Domain) sequence, which anchors the tetrameric form of the AChET in the plasma membrane of neurons in the synapse [36].

All models were built using the Modeller v9.20 [37]. Then, the quality of the models was analyzed by the Ramachandran plot generated by PROCHECK [38] and Molprobit [39] programs and the ERRAT web server [40].

2.3.2. Electrostatic profile

An important analysis in the process of structure-based drug design is the electrostatic profile. This analysis allows verifying the distribution of the electric charges in the protein molecular surface, being able to identify regions with a higher concentration of positive charges, as well as those with a higher level of negative charges. In this study, we used PDB2PQR v2.1 and APBS v1.5 softwares to calculate the charge distributions and generate the electrostatic profile.

2.3.3. ADMET analysis and target prediction

In silico analyzes on absorption, distribution, metabolism, excretion (ADME), and toxicity (T) has become an essential tool in rational drug design. Such analyzes have received considerable attention from pharmaceutical scientists, and various predictive models related to ADMET have been reported [41]. The high-throughput and low-cost nature of these models allow a more streamlined drug development process in which its structural optimization can be guided based on a parallel investigation of bioavailability and safety along with the activity. For the ADMET analysis, we used in this work the SwissADME [42].

Molecular target prediction was also made for each ligand to confirm AChE as a possible target. We used the SwissTargetPrediction [43] and Molinspiration servers for this analysis.

2.3.4. Molecular docking simulations

All ligands and control molecules were drawn in the ChemSketch software and their structures optimized in the Avogadro software v1.1, using the MMFF94 force field and the steepest descended algorithm. For docking simulations, the models were initially prepared by the addition of polar hydrogens and generation of pdbqt files in AutoDock Tools (ADT) v1.5.6. In the second step, the ligands (Table 2) and control molecules (physostigmine, resveratrol, and acetylcholine) were prepared in ADT, where the partial Gasteiger charges were added, rotatable bonds were set, and pdbqt files were generated.

The third step consisted in set as flexible a set of residues from the active site during the docking simulations, considering different classes of ligands found in PDB structures: (i) catalytic triad (HsAChET: E199, S200, H444; MmAChET: E202, S203, H447; EeAChET: E201, S202, H471); (ii) peripheric anionic site, also known as PAS (EeAChET: Y71, D73, Y123, W281, Y336; MmAChET: Y72, D74, Y124, W286, Y34; HsAChET, Y69, D71, Y121, W283, Y338); (iii) oxyanion hole (EeAChET: G120, G121, A203; MmAChET: G121, G122, A206; HsAChET: G118, G119, A201); and (iv) acyl pocket (EeAChET: F290, F292; F333; MmAChET, F295, F297; F338; HsAChET: F292, F294, F335).

For all the residues listed above, all bonds were allowed to be rotatable. The exceptions were residues Y71, D73, Y123, F292 for EeAChET; Y72, D74, Y124, W283, F294 for MmAChET; and Y69, D71, Y121, W283, F294 for HsAChET, where rotation between the alpha and beta carbons were disabled to maintain the maximum number of rotations allowed by AutoDock Vina.

The last step consists of setting in chain A, of both models, the center and size of the grid box. The center coordinates for EeAChET were X=-11, Y=-7, Z=56, with box sizes X=27Å, Y=28Å, and Z=24Å. The center coordinates for MmAChET were X=-14, Y=-10, Z=58, and box sizes X=20Å, Y=30Å, Z=22Å. For HsAChET, the center coordinates were X=-22, Y=-11, and Z=57, with box size X=18Å, Y=32Å, and Z=24Å.

Molecular docking was performed with AutoDock Vina [44]. As the AChE catalytic site presents five structural water molecules, an adaptation was necessary for the program AutoDock Vina. This adaptation consisted of including the parameters of the water molecule, similar to presented in Autodock Hydrated, in the AutoDock Vina parameter file.

2.4. *In vitro* AChE inhibitory assay

The RSV analogues were tested for AChE inhibiting activity using a modified Ellman's colorimetric method [45]. A 50 mM Tris-HCl pH 8.0 buffer was prepared for the assay. In 96-well plates, were added 25 µL of 15 mM AChI in water, 125 µL of 3 mM DTNB, 50 µL of the buffer, and 25 µL of the tested molecules dissolved in MeOH at concentrations ranging from 62.5 to 1000 µg mL⁻¹. Then, 25 µL of AChE solution (0.22 U mL⁻¹) was added, and the absorbance measured in a spectrophotometer (SpectraMax 190, Molecular Devices, Sunnyvale, CA, USA) at a wavelength of 415 nm every 15 seconds for 41 cycles at 37 °C. To avoid false-positive results, a parallel test omitting the DTNB was done. Physostigmine was used as a positive control. All assays were performed in triplicate. The percentage of inhibition was calculated using the following equation:

$$\% \text{ Inhibition} = [(E - S)/S] \times 100$$

where E is the enzyme activity without the test compound, and S is the enzyme activity with the tested compound. IC₅₀ for all analogues was determined using nonlinear regression in Graph Pad Prism version 6.0 for Windows, Graph Pad Software (San Diego, CA, USA), and it represents in which concentration the hydrolysis of acetylcholine is inhibited in 50%.

2.5. *In vivo* studies

2.5.1. Animals

This study was approved by the Ethics Committee on Animal Use (CEUA) of the Federal University of Santa Catarina (Florianópolis, Brazil) under the number 3914220319 for the LPS-induced depressive and scopolamine-induced amnesia models. The breeding unit of the same university provided the male Swiss mice (40-55 g, 8-week old). The animals were maintained under controlled light (07:00 a.m. to 07:00 p.m.), and temperature (21 ± 1 °C) conditions, and they were allowed to access standard food and water freely. All animal manipulations have occurred between 9:00 a.m. and 4:00 p.m. For this study, all procedures were performed according to the National Institute of Health Guidelines for Laboratory Care and Use. All efforts were made to minimize animal suffering and reduce the number of animals used in the experiment.

2.5.2. Experimental design

Scopolamine-induced amnesia model: for the scopolamine-induced amnesia model, male Swiss mice were randomly divided into four experimental groups: i) naive; ii) scopolamine (1 mg kg^{-1}), iii) RSVA6 (100 mg kg^{-1}) and iv) rivastigmine (1 mg kg^{-1}). RSVA6 (100 mg kg^{-1} , p.o.) and rivastigmine (1 mg kg^{-1} , i.p.) group animals were treated one hour before scopolamine administration (1 mg kg^{-1} , i.p.). Thirty minutes later, the mice were behaviorally analyzed by object recognition, object relocation, locomotor activity, and buried pellet tests [46,47].

LPS-induced depressive model: for the LPS-induced depressive model, the animals were randomly assigned to five experimental groups ($n = 5$ animals/group) to evaluate the RES analogue RSVA6 antidepressant-like behavior. LPS (0.5 mg kg^{-1}) was administered intraperitoneally, and 24 h after the injection, mice were treated with RSVA6 (1, 10, and 100 mg kg^{-1} , p.o.) or imipramine (20 mg kg^{-1} , i.p.). One hour later, the animals were behaviorally analyzed via the open field, tail suspension, and splash tests.

2.6. Memory and behavioral tests

2.6.1. Open Field Test (OFT)

The OFT was performed before the TST and ST trials, to evaluate the effect on locomotor and exploratory activities. For the test, a wooden box (40 cm x 60 cm x 50 cm) was used. Its floor was divided into 12 squares, and temperature, light, and noise were controlled. Mice were placed in the left corner of the field, with permission to freely explore the floor. The number of crossings (squares crossed by the animal with its four legs) and the number of rearing (animal standing upright on its riding paws) were registered throughout 6 minutes. At the end of each session, the floor was cleaned with a 10% ethanol solution [48].

2.6.2. Novel object recognition (NOR)

In the experimental protocol, the animals' memory of recognition is evaluated. Long habituation consists of three previous presentations on the apparatus. In this protocol, the animals were individually habituated in the open field for 5 minutes for three days. After 24 hours, they were again exposed to the arena with the presence of two equal objects placed on the floor, positioned in the same line, and with a distance of 7 cm on both sides of the box (training session). At this moment, we recorded the investigation time (in seconds) of each of the objects placed in the apparatus. The animals were removed from the open field, and after 24 hours, they were again exposed to the arena but replacing one object. Again, we record the exploration time (in seconds) of each of the objects placed in the box. The following are considered exploration of the object: smelling, touching, or observing the object less than 2 cm away [49,50]. For each animal, recognition memory was assessed via the discrimination index (DI; %), calculated as follows: $DI = TN / (TN + TF) \times 100$ [TN = time spent exploring the novel object; TF = time spent exploring the familiar object].

2.6.3. Object location test (OLT)

The object location memory test is used to test local memory in mice [51]. The animals underwent one day of habituation in the open field apparatus for 5 minutes. On day 2 of the protocol, the rodents were trained for 5

minutes in the arena with the presence of two equal objects, positioned 12 cm from each other and 11 cm from the wall. On day 3 (test day), one of the objects was moved from its original position to a new location, and the animals allowed to explore for 5 minutes. Moreover, we place visual clues on the walls for the animals. All objects were sanitized at each test to minimize olfactory cues between tests. They are considered as an exploration of the object: smelling, touching, or observing the object less than 2 cm away. As in the NOR, recognition memory was evaluated via DI (%). The locomotor activity was analyzed together with the object relocation test since the same apparatus was used for both tests.

2.6.4. Buried Pellet test (BPT)

In the experimental protocol, we evaluated the memory and olfactory capacity of the animals, 48 hours before the test each animal had its weight recorded and then underwent a dietary restriction at 90% of body weight. Before the test and during food restriction, each animal was offered two cereal pellets to be used in the test. The animals were fasted for 18 hours before training, followed by 1 hour of habituation in the room where the test took place. The test cage was prepared with 3 cm of fresh litter, with a cereal buried 0.5 cm below in one corner of the cage. Individually the animals were placed in the cage, and latency time is counted until the animal finds the sediment. If it does not find in the predetermined period of 300 seconds, the experiment ends, and a latency of 5 minutes will be recorded. The following day (24 hours after), the same training protocol was performed [52-54].

2.6.5. Tail Suspension Test (TST)

The TST is based on suspending the animals 50 cm above the ground by adhesive tape placed 1 cm from the tip of their tail, in an acoustically and visually isolated place. The immobility time was recorded throughout 6 minutes. The depressive-like behavior status is attributed to those mice that develop an apathetic and immobile posture when subjected to the short-term stress of being suspended by their tail [17].

2.6.6. Splash Test (ST)

The ST consists of spraying a 10% sucrose solution on the dorsal coat of the mice, and then they are put in a glass chamber. The sucrose solution dirties the mice's fur, and it leads the animals to initiate grooming behavior. The latency to begin the grooming was recorded for 5 minutes and used as a measure of self-care and motivational behavior. A grooming time decrease is associated with anhedonia and depressive-like behavior. After each session, the chamber was cleaned with a 10% ethanol solution [55].

2.6.7. Statistical analysis

All *in vivo* experimental results are expressed as the mean \pm standard error of the mean (SEM). The one-way and two-way analysis of variance (ANOVA) was performed to analyze the differences among experimental groups, and $P < 0.05$ was defined as statistically significant. The statistical analysis was achieved through Graph Pad Prism software version 6.0 for Windows, Graph Pad Software (San Diego, CA, USA).

3. RESULTS

3.1. Chemistry

The synthesis of the RSVA analogues has been carried out as previously described by Paula *et al.* [28] through condensation of aniline (1 mM) with several different aromatic aldehydes (1.1 mM), using ethanol as solvent. The reaction was allowed to stand at room temperature and constant stirring. After 0.5 to 24 hours, depending on the aldehyde, the compounds were obtained in solid form after the precipitate formed was filtered, washed in ethanol and dried in an oven.

3.2. *In silico* studies

3.2.1. AChET models

The models of MmAChET, HsAChET, and EeAChET are homotetramers formed by two antiparallel homodimers (AB and CD), and the monomers of each dimer are non-planar. The C-terminal region of each monomer in all models is complete and forms a helix around the PRAD sequence (Fig. 1).

The amino acid sequence of HsAChET shows a high identity and similarity with MmAChET (89% and 93%, respectively) and EsAChET (60% and 74%, respectively). Similarly, the amino acid sequence alignment between MmAChET and EeAChET also presents a high identity (60%) and similarity (71%). Alignments can be visualized in Supplementary Fig. 1.

These values of identity and similarity point to high structural conservation between the three enzymes, mainly between MmAChET and HsAChET. Such structural conservation is reflected in the similarity between the profiles of the electrostatic potentials on the outer surface of the three enzymes (Supplementary Fig. 2). The predominance of electronegative areas has already been highlighted by other works [56,57] as an important characteristic of AChE.

Structural conservation can also be observed among the residues that form the active site and gorge site of the studied enzymes. The list of residues, according to Lushington *et al.* [58] and Cheng *et al.* [59], is presented below following the order of EeAChET/MmAChET/HsAChET: (i) active site: Y71/ Y72/ Y69, D73/ D74/ D71, G120/ G121/ G118, G121/ G122/ G119, Y132/ Y133/ Y130, A203/ A204/ A201, F290/ F295/ F292, E329/ E334/ E331, Y332/ Y337/ Y334; (ii) gorge site: W85/ W86/ W83, Y123/ Y124/ Y121, W281/ W286/ W283, F292/ F297/ F294, F333/ F338/ F335, Y336/ Y341/ Y338; and catalytic triad: E201/ E202/ E199, S202/ S203/ S200, H471/ H447/ H444. This full conservation has an important consequence concerning the electrostatic profile of the active site that has a predominance of electronegative potential (Fig. 2).

Throughout the 3D modeling of AChET structures, six water molecules were maintained in the active site. These water molecules were selected based on the structural alignment of the templates and based on the literature [60].

3.2.2. Molecular docking simulations

The docking results presented in Table 2 include the binding energy of the compounds, the theoretical concentration of each compound required to produce half-maximum inhibition of the enzyme (cKi, based on the binding energy), and the description of the interactions between compounds and residues of AChE from *E. electricus*, *M. musculus*, and *H. sapiens*. Figure 3 shows all ligands best pose in the catalytic site of EeAChET (Fig. 3a), MmAChET (Fig. 3b), and HsAChET (Fig. 3c).

The RSV analogues interact with residues of histidine and serine from the catalytic triad, tyrosine, and tryptophan of PAS, and tryptophan of choline-binding site (Table 2 and Fig. 3). It is important to note that even considering the flexibility of some residues, all docking results of physostigmine in EeAChET presented conformations in the external binding site (Fig. 3a).

The consensus result of three organisms suggesting that the modifications made in the molecules resulted in ligands more potent than resveratrol, and point out RSVA1 and RSVA6 as potent inhibitors. A single docking image was prepared for these two compounds in the three organisms to compare the results (Fig. 4).

3.2.3. ADME predictions

SwissADME and Molinspiration were able to provide a significant amount of data on each compound analyzed. However, the most critical data are the parameters contained in Lipinski's rule of five (RO5) and the total polar surface area (TPSA). The results presented in Table 3 show that all compounds presented in this work follow the RO5, which indicates as minimal the probability of having dissolution and permeation problems. Comparing RSV and its analogues, the proposed compounds presented similar or even better values than the polyphenol.

3.3. The inhibitory effect of RSV analogues on AChE activity

All RSV derivatives were screened for AChE inhibitory capacity through Ellman's method with minor modifications [45] and classified according to their percentage of AChE inhibition [61] as potent (>50% inhibition), moderate (30-50% inhibition) or inactive/low activity (<30% inhibition). In sequence, the molecules were further investigated to determine their IC₅₀ values (Table 4).

Considering the analogue RSVA6 presented the best result in docking tests with *M. musculus*, and *in vitro* results pointed to this compound as the most potent AChET inhibitor of *E. electricus*, we elected RSVA6 to follow in the *in vivo* experiments.

3.4. Effects of acute treatment with RSVA6 on memory and behavioral assessments

3.4.1. RSVA6 has a neuroprotective effect on memory in the NOR, OLT, and BPT and does not affect locomotor activity

The NOR and OLT were conducted to assess the impact of RSVA6 on short-term (Fig. 5a, 5b), spatial memory (Fig. 5c, 5d) in scopolamine-induced amnesia. In the training phase, there were no significant differences

($P > 0.05$) in the discrimination index (DI) among groups in both NOR (Fig. 5a) and OLT (Fig. 5c). In the NOR test phase (Fig. 5b), the DI of the scopolamine groups was significantly reduced than that of the naïve group ($P < 0.01$). Contrarily, previous treatment with RSVA6 (100 mg kg⁻¹; p.o.) significantly elevated the DI ($P < 0.001$) compared to the scopolamine group, result as similar as that one observed to the rivastigmine group. The results from the OLT test phase (Fig. 5d) show a lower DI for the scopolamine group compared to the naïve group ($P < 0.05$). However, RSVA6 was significantly able ($P < 0.05$) to prevent memory impairment.

The BPT (Fig. 5e) evaluates the olfactory memory of mice. There were no significant differences among groups during the training phase ($P > 0.05$). In contrast, animals from the scopolamine group spent more time ($P < 0.01$) to find the buried pellet than those animals from the naïve group. However, RSVA6 lowered significantly ($P < 0.01$) the latency in comparison to the scopolamine group, indicating the neuroprotective effect of the RSV derivative. The OFT was applied to the animals from the scopolamine-induced amnesia model to exclude any suspect of locomotor impairment due to RSVA6 administration. There were no significant differences among groups (Fig. 5f).

3.4.2. LPS injection has no effect on the locomotor and exploratory activities, and RSVA6 has antidepressant-like behavior in the TST and ST

The OFT analyzed the number of crossing and rearing to discard a possible association between immobility in the behavioral tests and changes in motor activities. The one-way ANOVA revealed no significant alterations in the crossing number ($P > 0.05$) and the rearing number ($P > 0.05$; Fig. 6a and 6b, respectively), indicating that LPS has not affected either the locomotor and exploratory activities among groups. Consequently, the immobility time and anhedonia observed respectively in the TST and ST can be associated with depressive-like behavior.

The TST, one of the most commonly used tests for assessing antidepressant-like behavior in mice, was performed to evaluate the influence of RSVA6 (1, 10, and 100 mg kg⁻¹, p.o.) on the depressive-like behavior triggered by i.p. LPS (Fig. 6c and 6d). It was observed an increase in the immobility time in those animals exposed to LPS compared to the naïve group (Fig. 6c). The oral administration of RSVA6 at the highest dose (100 mg kg⁻¹, p.o.) has significantly reversed the LPS effect ($P < 0.01$). The same significant effect was observed in those animals treated with the standard drug (imipramine, mg kg⁻¹, i.p.). From the ST (Fig. 6e and 6f), LPS injection decreased the grooming time significantly when compared to the control group (Fig. 6e). The treatment with RSVA6 at the highest dose (100 mg kg⁻¹, p.o.) reversed this effect significantly ($P < 0.05$), as well as imipramine did. The results demonstrate an antidepressant-like action of the RES analogue RSVA6.

4. DISCUSSION

Herein, *in silico* studies carried out for RSV analogues have demonstrated the modifications made in the molecules resulted in structures more potent than RSV itself in the *in vitro* assay, which was able to point out RSVA1, RSVA3, and RSVA6 as potent inhibitors. The AChE active site is composed of three subsites: an anionic, a steric, and a peripheral anionic. In the first is located the catalytic site (serine-protease triad), the second is the site

of choline interaction, and the last one is the site of interaction of quaternary ligands [62]. The AChE mechanism of action consists of the following steps (Supplementary Fig. 3): (1) ACh approaches the site and a nucleophilic attack by serine hydroxyl group occurs; (2) an adjustment of electron configuration happens after the attack; (3) water is produced and leaves the Ser-ACh complex; (4) a nucleophilic attack by the water present in the site onto the acyl-enzyme, which will cause the deacylation of ACh; (5) and (6) shows the electron configuration where acetic acid is produced as the final product, and finally, residues return to the apo state [58]. RSV derivatives used in this study have a similar structure to acetylcholine, such as length, charged atoms, or electronegative atoms/groups at the second aromatic ring. They make the central region of the ring more positive, improving the chances of interactions with critical residues where "N⁺" from ACh interacts. Furthermore, the hydrogens at the first aromatic ring allow hydrogen bonds with the hydroxyl group from the catalytic serine. Comparing all the results, herein, the RSV interacts with essential residues for the mechanism of action of AChET, such as S200, from the catalytic triad and Y121, W283, and Y338, from PAS site (numbering according to *H. sapiens*). The strong interaction of these compounds, represented by very low binding energies, shows that these ligands probably compete with acetylcholine and prevent it from binding to the active site of AChET.

The ADME findings have demonstrated our RSV analogues as having a low probability of dissolution and permeation problems. According to RO5, a molecule has a higher chance of becoming a drug if there are no more than 5 hydrogens (H-) bond donors (sum of oxygen-hydrogen and oxygen-nitrogen bonds); no more than 10 H-bond acceptors (all nitrogen and oxygen); the molecular weight (MW) is less than 500 daltons, and LogP (octanol-water partition coefficient) is less than 5 [63]. The TPSA is used to evaluate drug transport properties. It is the sum of all surface areas of polar atoms (oxygen, nitrogen, and attached hydrogen), and it has shown a significant correlation with passive molecular transport through membranes and, therefore, it allows prediction of transport properties of drugs in the intestines and blood-brain barrier [64]. The TSPA value is inversely proportional to absorbance. Thus, values below 140 Å² favor intestine absorbance as long as values below 60 Å² favor blood-brain barrier absorbance [65]. Considering the brain as AChE local site, these results support our RSV analogues that presented values below 60 Å². It is important to note that RSV showed a value close to 60.7 Å² and that all the analogues tested had values below 60 Å². Respecting all the cited parameters, the chances of poor solubility and permeation and transportation impairments are less likely.

Dementia and depression are co-morbidities frequently observed in aged people, although the clinical relationship between both of them is poorly understood yet [66]. In AD, the most prevalent form of dementia in the elderly, downregulation of acetylcholine levels is one of the disease hallmarks [67] and correlated with illness severity [68]. Currently, searching for iAChEs is still a strategy to find an efficient treatment for AD since the few available drugs only alleviate the symptoms, in addition to presenting many side effects [69]. Following the *in silico* predictions, we have found analogues that showed higher AChE inhibitory capacity than RSV. RSVA6 had the best performance and made it to 92.4%, suggesting this compound as a good candidate for *in vivo* assessments.

In this present study, RSVA6 demonstrated a neuroprotective effect on scopolamine-induced memory impairments in mice. The olfactory memory was investigated via de BPT, and, as expected, the scopolamine

injection (1 mg kg⁻¹; i.p.) caused a sensory deficit in the animals even after a period of food deprivation. Both cholinergic receptor blockade and lesions in cholinergic projection neurons are capable of interfering with the acquisition of the olfactory associative memory [70]. Interestingly, olfactory dysfunction is commonly observed in the early stages of AD [71], and one of the causes may be the cholinergic deficit [72]. Although the efficacy (or not) of iAChE on olfactory dysfunction has not been elucidated yet, Velayudhan and Lovestone [73] demonstrated in an open study that donepezil therapy (5 - 10 mg/day; p.o.) was able to improve odor identification in AD patients, suggesting a higher ACh availability as playing a role on that enhancement. Thus, the results showed that pretreatment with RSVA6 (100 mg kg⁻¹; p.o.) exerted a neuroprotective effect on mice cognition, probably by inhibiting AChE and, consequently, increasing the ACh concentration at the brain regions involved in the olfactory processes.

The NOR and OLT tasks were used to assess the spatial and short-term recognition memory of the animals, taking into account their natural tendency to explore any novelty for longer than everyday items [74]. Animals from the ESC group (1 mg kg⁻¹; i.p.) were unable to distinguish both the object replaced in OLT and the object relocated in NOR from the familiar object. A significant reduction in DI compared to the control group was found, in agreement with previous studies [75-77]. Otherwise, the comparison between the RSVA6 and ESC groups showed a significant DI increase, suggesting a neuroprotective effect of the RSV analogue on the animals induced to cognitive impairment. The OFT was conducted to eliminate any interference on locomotor activities, which could be triggered by RSVA6 administration. No behavioral alterations were observed at all. Taken together, the *in silico*, *in vitro*, and *in vivo* data set indicates the RSVA6 neuroprotective action through blocking the enzyme AChE and, consequently, elevating the ACh concentration at the synaptic cleft during neuropathological processes. However, studies concerning the ACh and AChE levels after RSVA6 administration, as well as the molecule pharmacokinetics, are encouraged at this point.

Depressive signs or MDD occur in over 20% of the AD patients [78]. Previous observations have suggested an involvement of the cholinergic system in the depressive process, even though the mechanisms around this possible relationship are mostly unknown [79]. In a case-control study, Kamath and colleagues [80] found AChE levels significantly increased in patients who have been diagnosed with depression and had not received any treatment before the examination. The current drugs taken in the AD treatment are known to play a mild effect on depression, regardless of the observation of a connection between cognitive worsening and that psychiatric disorder [81]. From that perspective, RSVA6 significantly diminished the depressive signs developed on mice, and this result may have some relation to the molecule's ability to inhibit the AChE, even though the animal model here discussed is the LPS-induced instead of the scopolamine-induced. More tests are encouraged to investigate the mechanisms behind the results.

Another hypothesis suggested explaining the results found *in vivo* may be associated with the RSVA6 effect on the immune system. Inflammatory dysfunctions in both peripheral and central nervous systems have been correlated with psychiatric illness and neurodegeneration disorders like depression and AD [82-84]. A single LPS systemic challenge is well established as triggering acute systemic inflammation leading to behavioral changes in

animal models, being considered a model of intensification of MDD [85]. Endotoxin from gram-negative bacteria was previously identified as toll like receptor 4 ligand (TLR4) [86], and the signaling pathway activated via this receptor may generate neuroinflammation. TLR4 is a transmembrane protein [87] expressed at microglial cell surface [88]. The LPS-TLR4 binding mediates the activation of transcription factors, such as factor nuclear kappa B (NF- κ B), and consequently induces production and release of pro-inflammatory cytokines, like as the tumor necrosis factor (TNF) and interleukin (IL)-1 β [89]. Moreover, a previous report demonstrated that acute systemic LPS injection, besides elevating cytokines levels, increased microglial cells in different brain areas, including frontal cortex and hippocampus [90]. It means an exacerbation of the immune response triggered by the LPS model.

From the OFT, locomotor and exploratory activities among groups were not affected after LPS injection. Once it was established, the immobility time and anhedonia detected in the respective TST and ST were associated with depressive-like behavior. Previously, RSV has demonstrated to be able to reduce the release of pro-inflammatory factors, as well as the production of prostaglandins and the NF- κ B pathway [91-93], as illustrated in Figure 7. Recently, Finnell et al. [94] demonstrated *in vivo* a reduction of splenic cells expressing TNF and IL-1 β after a 12-day regimen with RSV (10 or 30 mg/kg/day i.p.). Furthermore, RSV decreased IL-1 β and TNF levels in the *locus coeruleus* of rats. This anti-inflammatory effect of RSV was previously attributed to its ability to downregulate TLR4 and NF- κ B p65 subunit expression with consequent reduction of cytokines levels [95-97]. In this present study, RSVA6 was effective in reversing the inflammatory response triggered by LPS. The observation that small bioactive molecules sharing structural similarities are more likely to share similar targets [43] points RSVA6 as a potential candidate for more studies exploring its effectiveness on neuroinflammatory pathways.

In summary, scientific evidence point to a relationship between neuroinflammation and a series of modifications in the brain that may be responsible for the onset of neurological and neuropsychiatric disorders. Moreover, the cholinergic system seems to be involved in several of those processes, even though little is known about the mechanisms behind the outbreak of diseases such as AD and MDD. Current pharmacological treatments are limited, which have either significant adverse effects or low efficacy. Therefore, natural compounds well-known as anti-inflammatory and immunomodulatory agents may prove useful as a new therapy or adjuvant to the strategies already taken to handle depression and AD, for example. Many *in vitro* and *in vivo* studies have demonstrated RSV as containing biological properties that could be advantageous to treat psychiatric and neurological patients. However, the clinical effects of RSV are impaired by its low bioavailability in humans [98]. Our set of RSV analogues have been shown through computational modeling as having similar or even better performance than RSV on dissolution and permeation. Most importantly, RSVA6 ability to inhibit AChE *in silico* and *in vitro* as well as the neuroprotective and anti-depressant effects observed *in vivo* made this RSV analogue a potent candidate to elucidate its molecular mechanisms of action more thoroughly.

Conflict of interest

The authors declare that there is no conflict of interest regarding the publication of this article.

Acknowledgments

The authors would like to thank the Brazilian agencies Coordenação de Aperfeiçoamento de Pessoal de Nível Superior (CAPES), Conselho Nacional de Desenvolvimento Científico e Tecnológico (CNPq), Fundação de Amparo à Pesquisa do Estado de Minas Gerais (FAPEMIG), and Universidade Federal de Juiz de Fora (UFJF). R.C.D. is a recipient of a research productivity fellowship from the CNPq.

REFERENCES

1. Franceschi C, Bonafè M, Valensin S, Olivieri F, De Luca M, Ottaviani E, De Benedictis G (2000) Inflamm-aging. An evolutionary perspective on immunosenescence. *Ann N Y Acad Sci* 908:244-54. <https://doi.org/10.1111/j.1749-6632.2000.tb06651.x>
2. Ventura MT, Casciaro M, Gangemi S, Buquicchio R (2017) Immunosenescence in aging: between immune cells depletion and cytokines up-regulation. *Clin Mol Allergy* 15:21. <https://doi.org/10.1186/s12948-017-0077-0>
3. Calabrese V, Santoro A, Monti D, Crupi R, Di Paola R, Latteri S, Cuzzocrea S, Zappia M, Giordano J, Calabrese EJ, Franceschi C (2018) Aging and Parkinson's Disease: Inflammaging, neuroinflammation and biological remodeling as key factors in pathogenesis. *Free Radic Biol Med* 115:80-91. <https://doi.org/10.1016/j.freeradbiomed.2017.10.379>
4. Beltrán-Castillo S, Eugenín J, von Bernhardt R (2018) Impact of Aging in Microglia-Mediated D-Serine Balance in the CNS. *Mediators Inflamm* 2018:7219732. <https://doi.org/10.1155/2018/7219732>
5. Zhang Y, Fan K, Liu Y, Liu G, Yang X, Ma J (2018) Cathepsin C Aggravates Neuroinflammation Involved in Disturbances of Behaviour and Neurochemistry in Acute and Chronic Stress-Induced Murine Model of Depression. *Neurochem Res* 43(1):80-91. <https://doi.org/10.1007/s11064-017-2320-y>
6. Leonoudakis D, Rane A, Angeli S, Lithgow GJ, Andersen JK, Chinta SJ (2017) Anti-Inflammatory and Neuroprotective Role of Natural Product Securinine in Activated Glial Cells: Implications for Parkinson's Disease. *Mediators Inflamm* 2017:8302636. <https://doi.org/10.1155/2017/8302636>
7. Paudel YN, Shaikh MF, Chakraborti A, Kumari Y, Aledo-Serrano Á, Aleksovska K, Alvim MKM, Othman I (2018) HMGB1: A Common Biomarker and Potential Target for TBI, Neuroinflammation, Epilepsy, and Cognitive Dysfunction. *Front Neurosci* 12:628. <https://doi.org/10.3389/fnins.2018.00628>
8. Costantini E, D'Angelo C, Reale M (2018) The Role of Immunosenescence in Neurodegenerative Diseases. *Mediators Inflamm* 2018: 6039171. <https://doi.org/10.1155/2018/6039171>
9. Del Pinto R, Ferri C (2018) Inflammation-Accelerated Senescence and the Cardiovascular System: Mechanisms and Perspectives. *Int J Mol Sci* 19(12):3701. <https://doi.org/10.3390/ijms19123701>
10. Subhi Y, Krogh Nielsen M, Molbech CR, Oishi A, Singh A, Nissen MH, Sørensen TL (2019) Plasma markers of chronic low-grade inflammation in polypoidal choroidal vasculopathy and neovascular age-related macular degeneration. *Acta Ophthalmol* 97(1):99-106. <https://doi.org/10.1111/aos.13886>
11. Liu Q, Chen Y, Shen C, Xiao Y, Wang Y, Liu Z, Liu X (2017) Chicoric acid supplementation prevents systemic inflammation-induced memory impairment and amyloidogenesis via inhibition of NF- κ B. *FASEB J* 31(4):1494-1507. <https://doi.org/10.1096/fj.201601071R>
12. Magalhães TNC, Weiler M, Teixeira CVL, Hayata T, Moraes AS, Boldrini VO, Dos Santos LM, de Campos BM, de Rezende TJR, Joaquim HPG, Talib LL, Forlenza OV, Cendes F, Balthazar MLF (2017) MAGALHÃES, T.N.C. et al. Systemic Inflammation and Multimodal Biomarkers in Amnesic Mild Cognitive Impairment and Alzheimer's Disease. *Mol Neurobiol* 55(7):5689-55697. <https://doi.org/10.1007/s12035-017-0795-9>
13. Hoskin JL, Al-Hasan Y, Sabbagh MN. Nicotinic Acetylcholine Receptor Agonists for the Treatment of Alzheimer's Dementia: An Update. *Nicotine Tob Res.* 2019;21(3):370–376. doi:10.1093/ntr/nty116
14. Ibrahim MM, Gabr MT. Multitarget therapeutic strategies for Alzheimer's disease. *Neural Regen Res.* 2019;14(3):437–440. doi:10.4103/1673-5374.245463
15. Byrne ML, Whittle S, Allen NB (2016). The Role of Brain Structure and Function in the Association Between Inflammation and Depressive Symptoms. *Psychosomatic Medicine*, 78(4), 389–400. doi:10.1097/psy.0000000000000311

16. Kumar A, Singh A, Ekavali (2015) A review on Alzheimer's disease pathophysiology and its management: an update. *Pharmacol Rep* 67(2):195-203. <https://doi.org/10.1016/j.pharep.2014.09.004>
17. Machado DG, Neis VB, Balen GO, Colla A, Cunha MP, Dalmarco JB, Pizzolatti MG, Prediger RD, Rodrigues AL (2012) Antidepressant-like effect of ursolic acid isolated from *Rosmarinus officinalis* L. in mice: evidence for the involvement of the dopaminergic system. *Pharmacol Biochem Behav* 103(2):204-211. <https://doi.org/10.1016/j.pbb.2012.08.016>
18. Manosso LM, Moretti M, Ribeiro CM, Gonçalves FM, Leal RB, Rodrigues ALS (2015) Antidepressant-like effect of zinc is dependent on signaling pathways implicated in BDNF modulation. *Prog Neuropsychopharmacol Biol Psychiatry* 59:59-67. <https://doi.org/10.1016/j.pnpbp.2015.01.008>
19. Freires IA, Sardi JCO, de Castro RD et al (2017) Alternative Animal and Non-Animal Models for Drug Discovery and Development: Bonus or Burden? *Pharm Res* 34: 681-686. <https://doi.org/10.1007/s11095-016-2069-z>
20. Bhuvanendran S, Kumari Y, Othman I, Shaikh MF (2018) Amelioration of Cognitive Deficit by Embelin in a Scopolamine-Induced Alzheimer's Disease-Like Condition in a Rat Model. *Front Pharmacol* 9(655):1-12. <http://dx.doi.org/10.3389/fphar.2018.00665>
21. Kouémou NE, Taiwe GS, Moto FCO, Pale S, Ngoupaye GT, Njapdounke JSK, Nkantchoua GCN, Pahaye DB, Bum EM (2017) Nootropic and Neuroprotective Effects of *Dichrocephala integrifolia* on Scopolamine Mouse Model of Alzheimer's Disease. *Front Pharmacol* 8(847):1-10. <http://dx.doi.org/10.3389/fphar.2017.00847>.
22. Qin L, Wu X, Block ML, Liu Y, Breese GR, Hong JS, Knapp DJ, Crews FT (2007) Systemic LPS causes chronic neuroinflammation and progressive neurodegeneration. *Glia* 55:453-462. <https://doi.org/10.1002/glia.20467>
23. Oliveira-Lima OC, Carvalho-Tavares J, Rodrigues MF, Gomez MV, Oliveira ACP, Resende RR, Gomez RS, Vaz BG, Pinto MCX (2019) Lipid dynamics in LPS-induced neuroinflammation by DESI-MS imaging. *Brain Behav Immun pii: S0889-1591(18)30639-1*. <https://doi.org/10.1016/j.bbi.2019.01.029>
24. Wang YW, Zhou Q, Zhang X, Qian QQ, Xu JW, Ni PF, Qian YN (2017) Mild endoplasmic reticulum stress ameliorates lipopolysaccharide-induced neuroinflammation and cognitive impairment via regulation of microglial polarization. *J Neuroinflammation* 14:233. <https://doi.org/10.1186/s12974-017-1002-7>
25. Sawda C, Moussa C, Turner RS (2017) Resveratrol for Alzheimer's disease. *Ann N Y Acad Sci* 1403(1): 142-149. <https://doi.org/10.1111/nyas.13431>
26. Varoni EM, Lo Faro AF, Sharifi-Rad J, Iriti M (2016) Anticancer Molecular Mechanisms of Resveratrol. *Front Nutr* 3:8. <https://doi.org/10.3389/fnut.2016.00008>
27. Riba A, Deres L, Sumegi B, Toth K, Szabados E, Halmosi R (2017) Cardioprotective Effect of Resveratrol in a Postinfarction Heart Failure Model. *Oxid Med Cell Longev* 2017:6819281. <https://doi.org/10.1155/2017/6819281>
28. Paula DTS, Carvalho GSG, Almeida AC, Lourenço M, Silva AD, Coimbra ES (2013) Synthesis, Cytotoxicity and Antileishmanial Activity of Aza-Stilbene Derivatives. *Med J Chem* 2(3):493-502. <http://dx.doi.org/10.13171/mjc.2.3.2013.07.02.16>
29. Silva AD, Dos Santos JA, Machado PA, Alves LA, Laque LC, de Souza VC, Coimbra ES, Capriles PVSZ (2018) Insights about resveratrol analogues against trypanothione reductase of *Leishmania braziliensis*: molecular modeling, computational docking and in vitro antileishmanial studies. *J Biomol Struct Dyn* 28:1-34. <https://doi.org/10.1080/07391102.2018.1502096>
30. Oliveira MR, Chenet AL, Duarte AR, Scaini G, Quevedo J (2018) Molecular Mechanisms Underlying the Anti-depressant Effects of Resveratrol: a Review. *Mol Neurobiol* 55(6):4543-4559. <https://doi.org/10.1007/s12035-017-0680-6>

31. Lange KW, Li S (2017) Resveratrol, pterostilbene, and dementia. *Biofactors* 44(1):83-90. <https://doi.org/10.1002/biof.1396>
32. Calil NO, de Carvalho GSG, Zimmermann Franco DCZ, da Silva AD, Raposo NRB (2012) Antioxidant Activity of Resveratrol analogues. *Lett Drug Des Discov* 9:1. <https://doi.org/10.2174/157018012798192928>
33. Franco DCZ, de Carvalho GSG, Rocha PR, Teixeira RS, da Silva AD, Raposo NRB (2012) Inhibitory Effects of Resveratrol analogues on Mushroom Tyrosinase Activity. *Molecules* 17:11816-11825. <https://doi.org/10.3390/molecules171011816>
34. Bourne Y, Taylor P, Bougist P E, Marchot P (1999a) Crystal structure of mouse acetylcholinesterase. A peripheral site-occluding loop in a tetrameric assembly. *J Biol Chem* 274(5):2963-70. <https://doi.org/10.1074/jbc.274.5.2963>
35. Bourne Y, Grassi J, Bougist P E, Marchot P (1999b) Conformational Flexibility of the Acetylcholinesterase Tetramer Suggested by X-ray Crystallography. *J Biol Chem* 274(43):30370-6. <https://doi.org/10.1074/jbc.274.43.30370>
36. Massoulié J, Bon S, Perrier N, Falasca C (2005) The C-terminal peptides of acetylcholinesterase: Cellular trafficking, oligomerization and functional anchoring. *Chem Biol Interact* 157-158:3-14. <https://doi.org/10.1016/j.cbi.2005.10.002>
37. Eswar N, Webb B, Marti-Renom MA, Madhusudhan MS, Eramian D, Shen MY, Pieper U, Sali A (2016) Comparative Protein Structure Modeling Using Modeller. *Curr Protocol Bioinformatics* 5:5-6. <https://doi.org/10.1002/0471250953.bi0506s15>
38. Laskowski RA, MacArthur MW, Moss DS, Thornton JM (1993) PROCHECK: a program to check the stereochemical quality of protein structures. *J Appl Cryst* 26(2):283-291. <https://doi.org/10.1107/S0021889892009944>
39. Davis IW, Leaver-Fay A, Chen VB, Block JN, Kapral GJ, Wang X, Murray LW, Arendall WB 3rd, Snoeyink J, Richardson JS, Richardson DC (2007) MolProbity: all-atom contacts and structure validation for proteins and nucleic acids. *Nucleic Acids Res* 35(Web Server issue):W375-83. <https://doi.org/10.1093/nar/gkm216>
40. Colovos C, Yeates TO (1993) Verification of protein structures: patterns of nonbonded atomic interactions. *Protein Sci* 2(9):1511-1519. <https://doi.org/10.1002/pro.5560020916>
41. Wang Y, Xing J, Xu Y, Zhou N, Peng J, Xiong Z, Liu X, Luo X, Luo C, Chen K, Zheng M, Jiang H (2015) *In silico* ADME/T modelling for rational drug design. *Q Rev Biophys* 48: 488–515. <https://doi.org/10.1017/S0033583515000190>
42. Daina A, Michielin O, Zoete V (2017) SwissADME: a free web tool to evaluate pharmacokinetics, drug-likeness and medicinal chemistry friendliness of small molecules. *Sci Rep* 7:42717. <https://doi.org/10.1038/srep42717>
43. Gfeller D, Grosdidier A, Wirth M, Daina A, Michielin O, Zoete V (2014) SwissTargetPrediction: a web server for target prediction of bioactive small molecules. *Nucleic Acids Res* 42:W32–W38. <https://doi.org/10.1093/nar/gku293>
44. Trott O, Olson AJ (2010) AutoDock Vina: Improving the speed and accuracy of docking with a new scoring function, efficient optimization, and multithreading. *J Comput Chem* 31(2): 455–461. *Journal of Computational Chemistry*, v.31, n.2, 2009. <https://dx.doi.org/10.1002%2Fjcc.21334>
45. Ellman GL, Courtney KD, Jr VA, Featherstone RM (1961) A new and rapid colorimetric determination of acetylcholinesterase activity. *Biochem. Pharmacol* 7(2):88–95. [https://doi.org/10.1016/0006-2952\(61\)90145-9](https://doi.org/10.1016/0006-2952(61)90145-9)
46. Pitsikas N (2007) Effects of scopolamine and l-NAME on rats' performance in the object location test. *Behav Brain Res* 179(2):294-298. Elsevier BV. <http://dx.doi.org/10.1016/j.bbr.2007.02.038>.
47. Verma L, Jain NS (2016) Central histaminergic transmission modulates the ethanol induced anxiolysis in mice. *Behav Brain Res* 313:38-52. <https://doi.org/10.1016/j.bbr.2016.07.012>

48. Zeni AL, Zomkowski AD, Maraschin M, Rodrigues AL, Tasca CI (2012) Ferulic acid exerts antidepressant-like effect in the tail suspension test in mice: evidence for the involvement of the serotonergic system. *Eur J Pharmacol* 679(1-3):68-74. <https://doi.org/10.1016/j.ejphar.2011.12.041>
49. Rodrigues AL, Rocha JB, Mello CF, Souza DO (1996) Effect of perinatal lead exposure on rat behavior in open field and two-way avoidance tasks. *Pharmacol Toxicol* 79(3):150 – 156. <https://doi.org/10.1111/j.1600-0773.1996.tb00259.x>
50. Yang Y, Cudaback E, Jorstad NL, Hemingway JF, Hagan CE, Melief EJ, Li X, Yoo T, Khademi SB, Montine KS, Montine TJ, Keene CD. APOE3, but Not APOE4, Bone Marrow Transplantation Mitigates Behavioral and Pathological Changes in a Mouse Model of Alzheimer Disease. *Am J Pathol.* 2013;183:905–917
51. Luine, VN, Jacome, LF e Maclusky, NJ (2003). Rapid improvement of visual and local memory by estrogen in rats. *Endocrinology* 144, 2836-2844. doi: 10.1210 / pt.2003-0004
52. Yang Mu, Cawley JN (2009) Simple Behavioral Assessment of Mouse Olfaction. *Curr Protoc Neurosci* 8:8-24. <https://doi.org/10.1002/0471142301.ns0824s48>
53. Leger M, Quiedeville A, Bouet V et al (2013) Object recognition test in mice. *Nat Protoc* 8:2531–2537. <https://doi.org/10.1038/nprot.2013.155>
54. Lehmkuhl AM, Dirr ER, Fleming SM (2014) Olfactory Assays for Mouse Models of Neurodegenerative Disease. *J Vis Exp* (90):e51804. <https://doi.org/10.3791/51804>
55. Lieberknecht V, Cunha MP, Junqueira SC, Coelho ID, de Souza LF, Dos Santos AR, Rodrigues AL, Dutra RC, Dafre AL (2017) Antidepressant-like effect of pramipexole in an inflammatory model of depression. *Behav Brain Res* 320:365-373. <https://doi.org/10.1016/j.bbr.2016.11.007>
56. Botti SA, Felder CE, Sussman JL, Silman I (1998) Electrotactins: a class of adhesion proteins with conserved electrostatic and structural motifs. *Protein Eng* 11(6):415-420. <https://doi.org/10.1093/protein/11.6.415>
57. Felder CE, Botti SA, Lifson S, Silman I, Sussman JL (1997) External and internal electrostatic potentials of cholinesterase models. *J Mol Graph and Model* 15:318-327. [https://doi.org/10.1016/S1093-3263\(98\)00005-9](https://doi.org/10.1016/S1093-3263(98)00005-9)
58. Lushington GH, Guo J-X, Hurley MM (2006) Acetylcholinesterase: Molecular Modeling with the Whole Toolkit. *Curr Top Med Chem* 6:57-73. <https://doi.org/10.2174/156802606775193293>
59. Cheng S, Song W, Yuan X, Xu Y (2017) Gorge Motions of Acetylcholinesterase Revealed by Microsecond Molecular Dynamics Simulations. *Sci Rep* 7:3219. <https://dx.doi.org/10.1038%2Fs41598-017-03088-y>
60. Lopes JPB, Costa JS, Ceschi MA, Gonçalves CAS, Konrath EL, Karl ALM, Guedes IA, Dardenne LE (2017) Chiral Bistacrine analogues: Synthesis, Cholinesterase Inhibitory Activity and a Molecular Modeling Approach. *J Braz Chem Soc* 28(11): 2218-2228. <http://dx.doi.org/10.21577/0103-5053.20170074>
61. Vinutha B, Prashanth D, Salma K, Sreeja SL, Pratiti D, Padmaja R, Radhika S, Amit A, Venkateshwarlu K, Deepak M (2007) Screening of selected Indian medicinal plants for acetylcholinesterase inhibitory activity. *J Ethnopharmacol* 109(2):359-63. <https://doi.org/10.1016/j.jep.2006.06.014>
62. Dvir H, Silman I, Harel M, Rosenberry TL, Sussman JL (2010) Acetylcholinesterase: From 3D structure to function. *Chem Biol Interact* 187(1-3):10-22. <https://doi.org/10.1016/j.cbi.2010.01.042>
63. Lipinski CA, Lombardo F, Dominy BW, Feeney PJ (2001) Experimental and computational approaches to estimate solubility and permeability in drug discovery and development settings. *Adv Drug Deliv Rev* 46(1-3):3-26. [https://doi.org/10.1016/S0169-409X\(00\)00129-0](https://doi.org/10.1016/S0169-409X(00)00129-0)

64. Ahsan MJ, Samy JG, Khalilullah H, Nomani MS, Saraswat P, Gaur R, Singh A (2011) Molecular properties prediction and synthesis of novel 1,3,4-oxadiazole analogues as potent antimicrobial and antitubercular agents. *Bioorg Med Chem Lett* 21(24):7246-50. <https://doi.org/10.1016/j.bmcl.2011.10.057>
65. Prasanthi G (2014) In-silico estimation on oral bioavailability and drug-likeness of mono and bis-mannich bases of piperazine derivatives. *JGTPS* 5(1):1485-1488.
66. Bennett S, Thomas AJ (2014) Depression and dementia: cause, consequence or coincidence? *Maturitas* 79(2):184-90. <https://doi.org/10.1016/j.maturitas.2014.05.009>
67. Fotiou D, Kaltsatou A, Tsiptsios D, Nakou M (2015) Evaluation of the cholinergic hypothesis in Alzheimer's disease with neuropsychological methods. *Aging Clin Exp Res* 27(5):727-33. <https://doi.org/10.1007/s40520-015-0321-8>
68. Lanctôt KL, Herrmann N, LouLou MM (2003) Correlates of response to acetylcholinesterase inhibitor therapy in Alzheimer's disease. *J Psychiatry Neurosci* 28(1): 13–26.
69. Hung SY, Fu WM (2017) Drug candidates in clinical trials for Alzheimer's disease. *J Biomed Sci* 24:47. <https://doi.org/10.1186/s12929-017-0355-7>
70. Wilson DA, Fletcher ML, Sullivan RM (2004) Acetylcholine and Olfactory Perceptual Learning. *Learn Mem* 11(1):28-34. <https://doi.org/10.1101/lm.66404>
71. Lian TH, Zhu WL, Li SW et al (2019) Clinical, Structural, and Neuropathological Features of Olfactory Dysfunction in Patients with Alzheimer's Disease. *J Alzheimers Dis* 70(2):413-423. <https://doi.org/10.3233/JAD-181217>
72. Zou Y, Lu D, Liu L, Zhang H, Zhou Y (2016) Olfactory dysfunction in Alzheimer's disease. *Neuropsychiatr Dis Treat* 12:869-875. <https://dx.doi.org/10.2147%2FNDT.S104886>
73. Velayudhan L, Lovestone S (2009) Smell Identification Test as a Treatment Response Marker in Patients with Alzheimer Disease Receiving Donepezil. *J Clin Psychopharmacol* 29(4):387-390. <https://doi.org/10.1097/JCP.0b013e3181aba5a5>
74. Lu C, Wang Y, Wang D et al (2018) Neuroprotective Effects of Soy Isoflavones on Scopolamine-Induced Amnesia in Mice. *Nutrients* 10(7):853-876. <https://dx.doi.org/10.3390%2Fnu10070853>
75. Melamed JL, de Jesus FM, Maior RS, Barros M (2017) Scopolamine Induces Deficits in Spontaneous Object-Location Recognition and Fear-Learning in Marmoset Monkeys. *Front Pharmacol* 8(395):1-10. <https://dx.doi.org/10.3389%2Ffphar.2017.00395>
76. Sui Z, Qi C, Huang Y et al (2017) Aqueous extracts from asparagus stems prevent memory impairments in scopolamine-treated mice. *Food Funct* 8(4):1460-1467. <https://doi.org/10.1039/c7fo00028f>
77. Lu C, Wang Y, Xu T et al (2018) Genistein Ameliorates Scopolamine-Induced Amnesia in Mice Through the Regulation of the Cholinergic Neurotransmission, Antioxidant System and the ERK/CREB/BDNF Signaling. *Front Pharmacol* 9(1153):1-11. <https://doi.org/10.3389/fphar.2018.01153>
78. Richard E, Reitz C, Honig LH, Schupf N, Tang MX, Manly JJ, Mayeux R, Devanand D, Luchsinger JA (2013) Late-life depression, mild cognitive impairment, and dementia. *JAMA Neurol* 70(3):374-82. <https://doi.org/10.1001/jamaneurol.2013.603>
79. Mineur YS, Obayemi A, Wigstrand MB et al (2013) Cholinergic signaling in the hippocampus regulates social stress resilience and anxiety- and depression-like behavior. *Proc Natl Acad Sci U S A* 110(9):3573–3578. [doi:10.1073/pnas.1219731110](https://doi.org/10.1073/pnas.1219731110)

80. Kamath SU, Chaturvedi A, Bhaskar Yerrapragada D, Kundapura N, Amin N, Devaramane V (2019) Increased Levels of Acetylcholinesterase, Paraoxonase 1, and Copper in Patients with Moderate Depression- a Preliminary Study. *Rep Biochem Mol Biol* 7(2):174–180.
81. Jawaid A, Pawlowicz E, Schulz PE (2015) Do Acetylcholinesterase Inhibitors Increase Anxiety and Depression in Elderly Adults with Dementia? *J Am Geriatr Soc* 63(8):1702–1704. doi:10.1111/jgs.13567
82. Najjar S, Pearlman DM, Alper K, Najjar A, Devinsky O (2013) Neuroinflammation and psychiatric illness. *J Neuroinflammation* 10:43. <https://doi.org/10.1186/1742-2094-10-43>
83. Hong H, Kim BS, Im H (2016) Pathophysiological Role of Neuroinflammation in Neurodegenerative Diseases and Psychiatric Disorders. *Int Neurourol J* 20(Suppl 1):S2–7. <https://doi.org/10.5213/inj.1632604.302>
84. Schain M, Kreisl WC (2017) Neuroinflammation in Neurodegenerative Disorders-a Review. *Curr Neurol Neurosci Rep* 17(3):25. <https://doi.org/10.1007/s11910-017-0733-2>
85. Arioiz BI, Tastan B, Tarakcioglu E, et al (2019) Melatonin Attenuates LPS-Induced Acute Depressive-Like Behaviors and Microglial NLRP3 Inflammasome Activation Through the SIRT1/Nrf2 Pathway. *Front Immunol* 10:1511. doi:10.3389/fimmu.2019.01511
86. Beutler B (2000) Tlr4: central component of the sole mammalian LPS sensor. *Curr Opin Immunol* 12(1):20-26. [https://doi.org/10.1016/s0952-7915\(99\)00046-1](https://doi.org/10.1016/s0952-7915(99)00046-1)
87. Kuzmich N, Sivak K, Chubarev V et al (2017) TLR4 Signaling Pathway Modulators as Potential Therapeutics in Inflammation and Sepsis. *Vaccines* 5(4):34-59. <https://doi.org/10.3390/vaccines5040034>
88. Lehnardt S, Lachance C, Patrizi S et al (2002) The Toll-Like Receptor TLR4 Is Necessary for Lipopolysaccharide-Induced Oligodendrocyte Injury in the CNS. *J Neurosci* 22(7): 2478-2486. <https://doi.org/20026268>.
89. Zhao J, Bi W, Xiao S et al (2019) Neuroinflammation induced by lipopolysaccharide causes cognitive impairment in mice. *Sci Rep* 9(1). <https://doi.org/10.1038/s41598-019-42286-8>.
90. Noh H, Jeon L, Seo H (2014) Systemic injection of LPS induces region-specific neuroinflammation and mitochondrial dysfunction in normal mouse brain. *Neurochem Int* 69:35-40. <https://doi.org/10.1016/j.neuint.2014.02.008>.
91. Das S, Das DK (2007) Anti-Inflammatory Responses of Resveratrol. *Inflamm Allergy Drug Targets* 6(3):168-73. <https://doi.org/10.2174/187152807781696464>
92. Candelario-Jalil E, Oliveira ACP, Gräf S, Bhatia HS, Hüll M, Muñoz E, Fiebich BL (2007) Resveratrol potently reduces prostaglandin E2 production and free radical formation in lipopolysaccharide-activated primary rat microglia. *J Neuroinflammation* 4:25. <https://doi.org/10.1186/1742-2094-4-25>
93. Meng XL, Yang JY, Chen GL, Wang LH, Zhang LJ, Wang S, Li J, Wu CF (2008) Effects of resveratrol and its derivatives on lipopolysaccharide-induced microglial activation and their structure-activity relationships. *Chem Biol Interact* 174(1):51-9. <https://doi.org/10.1016/j.cbi.2008.04.015>
94. Finnell JE, Lombard CM, Melson MN, Singh NP, Nagarkatti M, Nagarkatti P, Fadel JR, Wood CS, Wood SK (2017) The protective effects of resveratrol on social stress-induced cytokine release and depressive-like behavior. *Brain Behav Immun* 59:147–157. <https://doi.org/10.1016/j.bbi.2016.0>
95. Feng Y, Cui Y, Gao J et al (2016) Resveratrol attenuates neuronal autophagy and inflammatory injury by inhibiting the TLR4/NF- κ B signaling pathway in experimental traumatic brain injury. *Int J Mol Med* 37(4):921-930. <https://doi.org/10.3892/ijmm.2016.2495>.

96. Wang G, Hu Z, Fu Q et al (2017) Resveratrol mitigates lipopolysaccharide-mediated acute inflammation in rats by inhibiting the TLR4/NF- κ Bp65/MAPKs signaling cascade. *Sci Rep* 7(1). <http://dx.doi.org/10.1038/srep45006>.
97. Lei J, Tu X, Wang Y et al (2019) Resveratrol downregulates the TLR4 signaling pathway to reduce brain damage in a rat model of focal cerebral ischemia. *Exp Ther Med* 17(4):3215-3221. <https://dx.doi.org/10.3892%2Fetm.2019.7324>.
98. Cottart CH, Nivet-Antoine V, Laguillier-Morizot C, Beaudoux JL (2010) Resveratrol bioavailability and toxicity in humans. *Mol Nutr Food Res* 54(1):7-16. <https://doi.org/10.1002/mnfr.200900437>

Scheme 1. Synthetic pathway of RSV analogues.

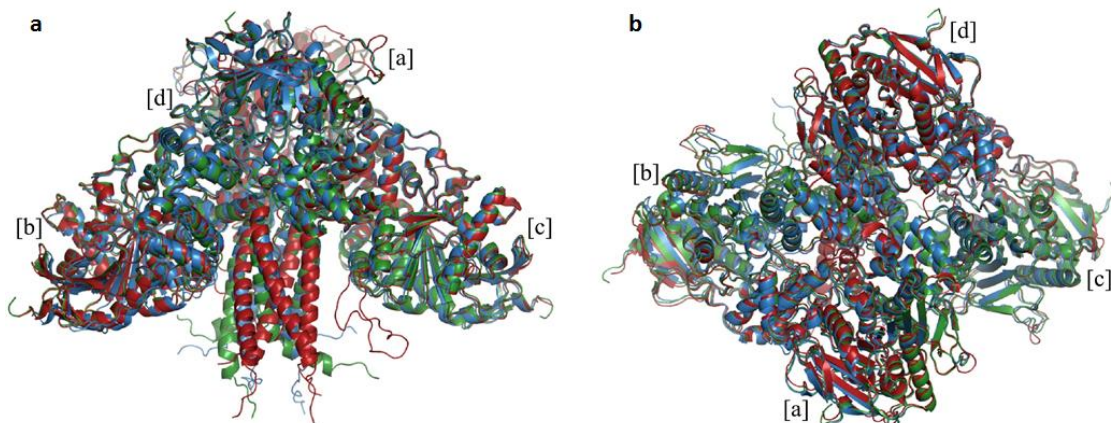
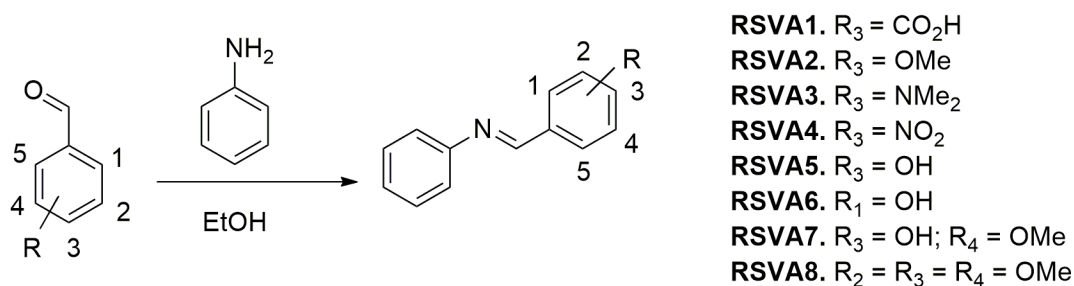


Figure 1: 3D model of tetrameric structure of MmAChET, HsAChET, and EeAChET. **(a)** Front view of structural alignment of models in cartoon representation: EeAChE-T (red), MmAChE-T (green), and HsAChE-T (blue). **(b)** Top view of chains.

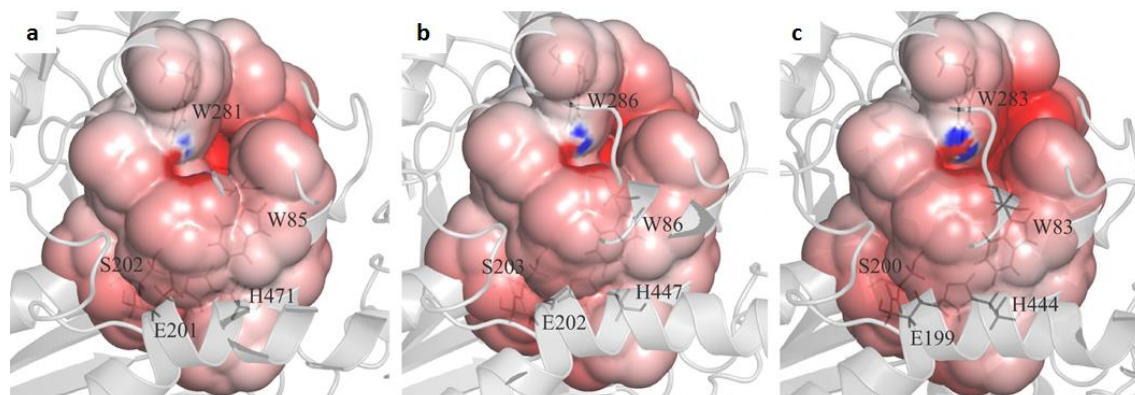


Figure 2: Electrostatic potential profile of the active site of acetylcholinesterase models: (a) EeAChE-T, (b) MmAChE-T and (c) HsAChE-T. The electrostatic potential profile of AChET vary from -5 (red) to 5 (blue) kT/e. The image was generated using PyMOL version 1.8.2, Schrödinger – LLC.

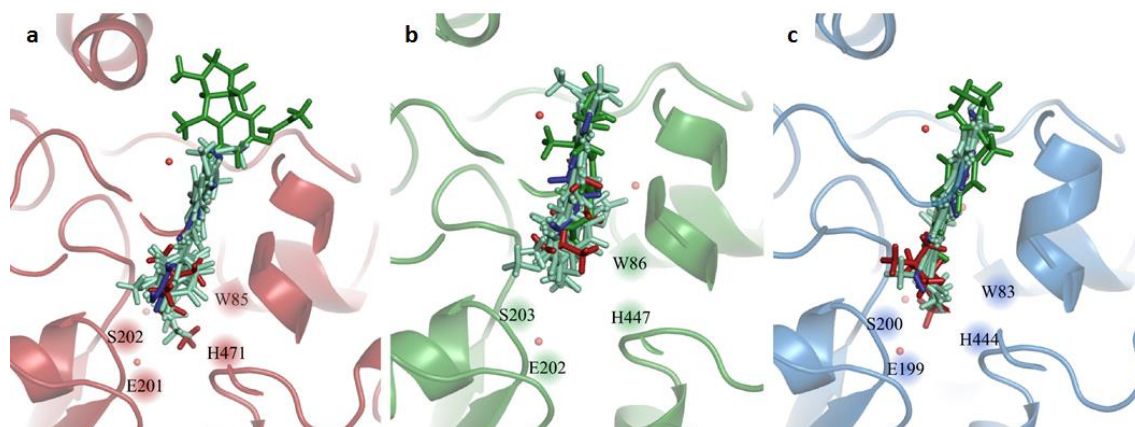


Figure 3: Binding mode for all ligands (best conformations): (a) EeAChET (red), (b) MmAChET (green), and (c) HsAChET (blue) in cartoon representation. Score values of each docking are presented in Table 2. Ligands are in stick representation: acetylcholine (red), physostigmine (green), resveratrol (blue), and resveratrol analogues (cyan). The main active site residues are highlighted by numbered spheres. The images were generated using PyMOL version 1.8.2, Schrödinger – LLC.

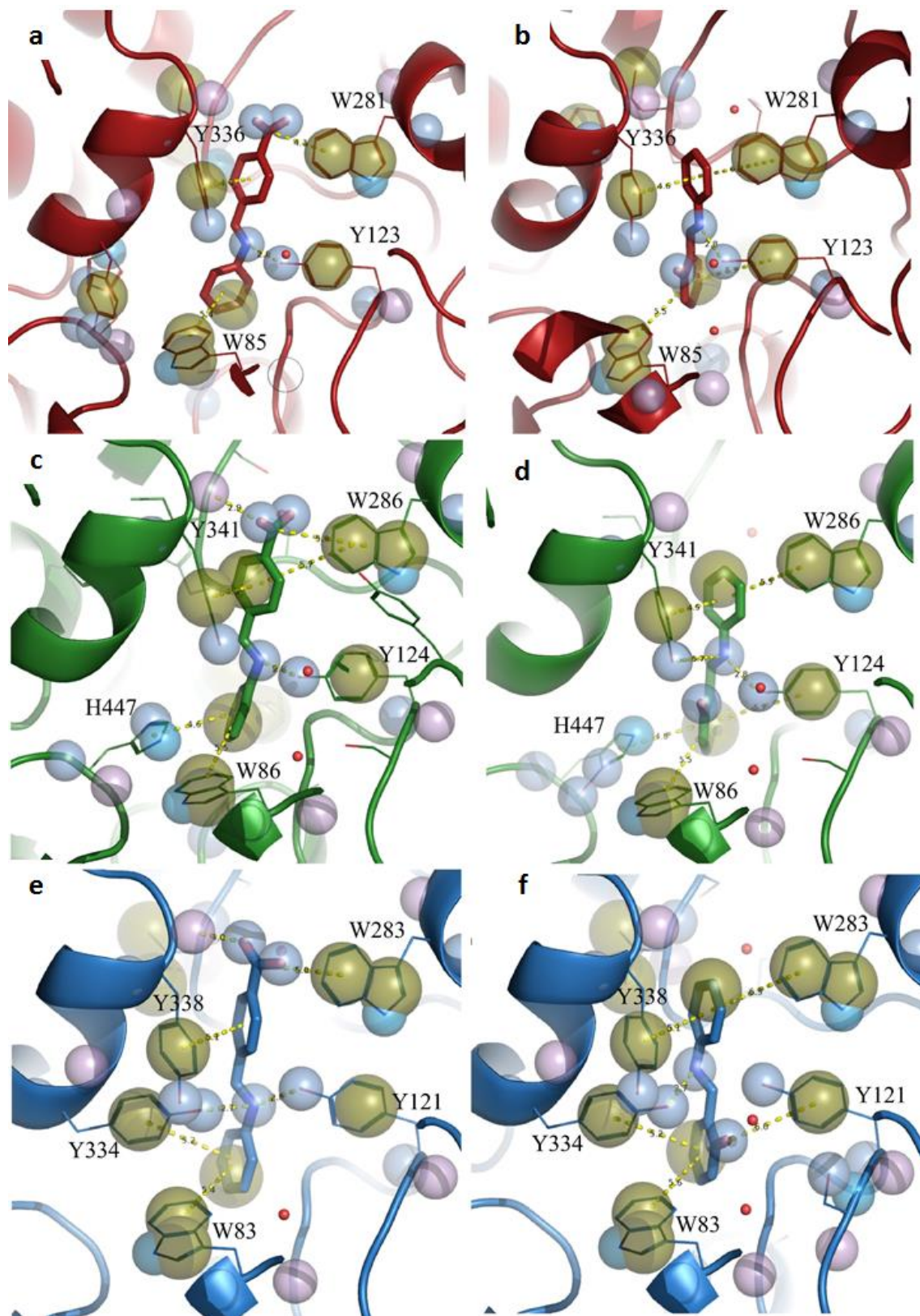


Figure 4: Best docking results of RSV analogues against acetylcholinesterase. Score values of each docking are presented in Table 2. The compounds RSVA1 (a, c, e) and RSVA6 (b, d, f) are in sticks representation and (a-b) EeAChET (red), (c-

d) MmAChET (green), and (e-f) HsAChET (blue) are in cartoon representation. Pharmacophoric characteristics are represented by spheres: aromatic ring and lipophilic region (gold), hydrogen bond donor (light blue), hydrogen bond acceptor (purple), hydrogen bond donor and acceptor (blue). The images were generated using PyMOL version 1.8.2, Schrödinger – LLC.

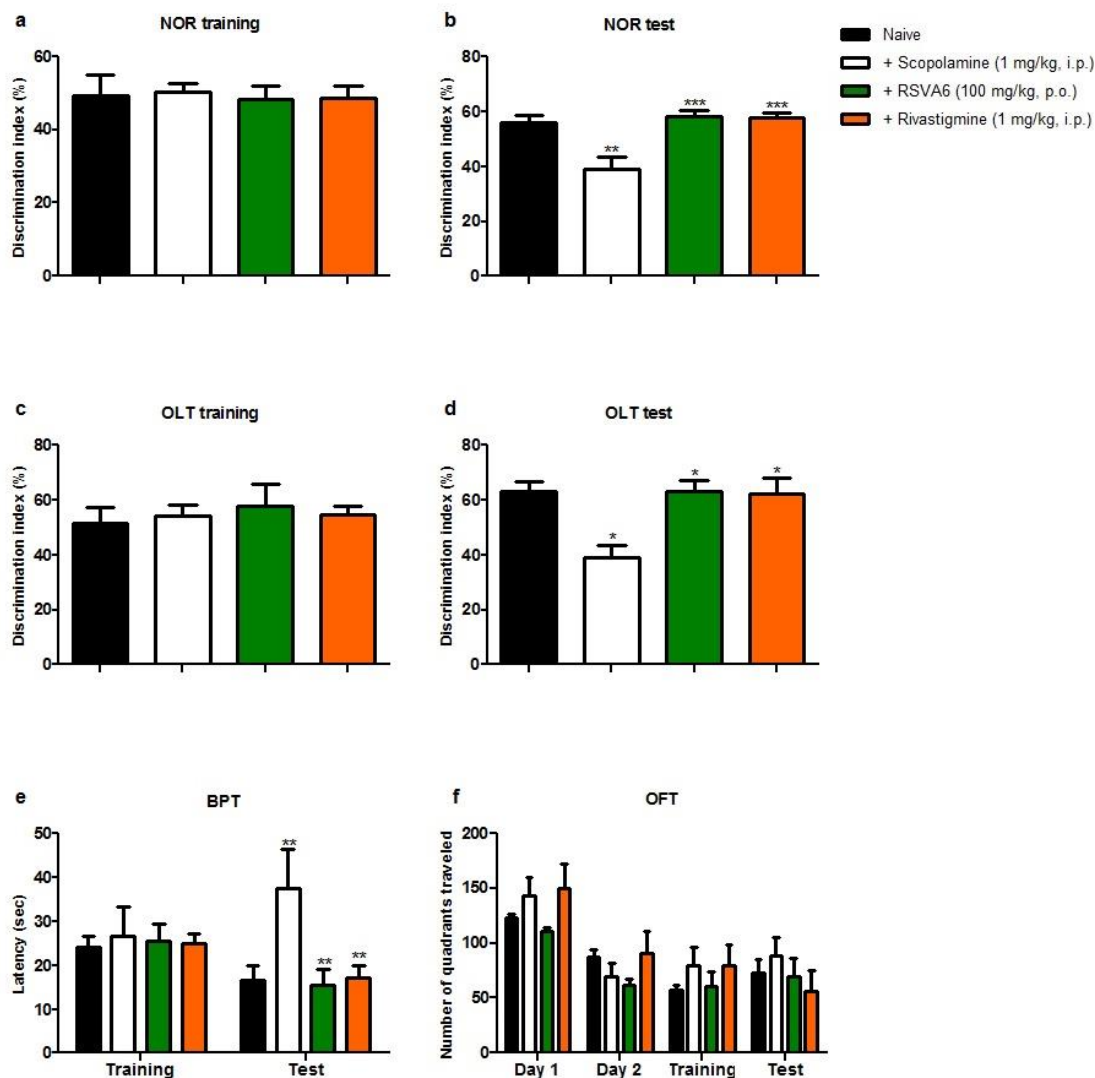


Figure 5: Effect of RSVA6 treatment using a scopolamine-induced amnesia model in mice. RSVA6 (100 mg kg⁻¹, p.o.) and rivastigmine (1 mg kg⁻¹, i.p.) were administered 60 minutes prior to scopolamine (1 mg kg⁻¹, i.p.) before the studies. Novel object recognition (NOR), object relocation (OLT), buried pellet test (BPT) and open field test (OFT) were completed. (a) discrimination index in object recognition test training, (b) discrimination index in object recognition test, (c) discrimination index in object location test training, (d) discrimination index in object location test, (e) latency in seconds to find pellet in the buried pellet test, (f) number of quadrants traveled in open field test. Data are expressed as mean \pm standard error of the mean. Statistical analysis was performed using two-way ANOVA by Bonferroni's *post-hoc* test. *P < 0.05, **P < 0.01, ***P < 0.001.

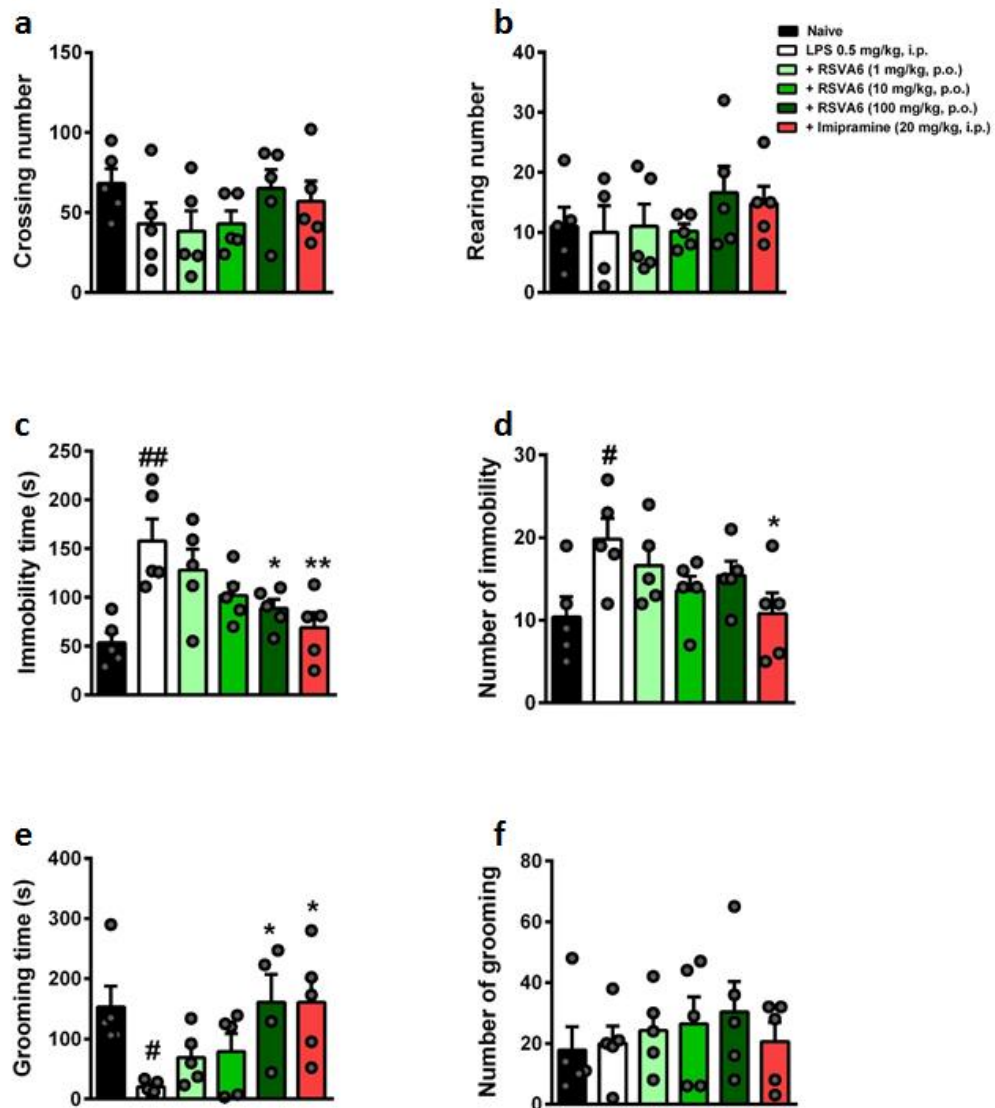


Figure 6:

Influence of **RSVA6** treatment on LPS-induced depressive-like behavior. (a) Crossing number and (b) rearing number in the OFT. (c) Immobility time and (d) number of immobility in the TST. (e) Grooming time and (f) number of grooming in the ST. Data are shown as *Mean*±*SEM*, n=5. #P < 0.05, ##P < 0.01 vs control; *P < 0.05, **P < 0.01 vs LPS.

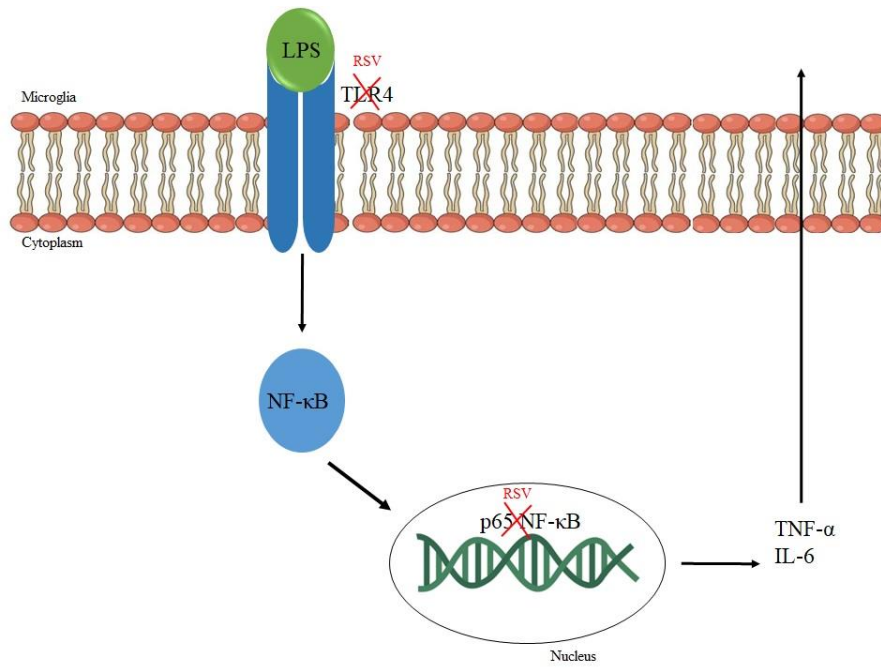


Figure 7: Schematic representation of resveratrol anti-inflammatory action on LPS-TLR4 signaling pathway.

Table 1: Spectral data of RSV analogues.

Compounds	δ CH=N	δ C=N	Melting Point (°C)	Yield (%)
RSVA1	8.72	159.8	220.4-221.6	67.0
RSVA2	8.51	159.8	61.4-62.1	65.0
RSVA3	8.39	159.9	96.8-97.3	72.0
RSVA4	8.80	158.8	89.6-90.7	75.0
RSVA5	8.44	160.0	89.2-90.7	74.0
RSVA6	8.96	163.5	50.7-51.4	63.0
RSVA7	8.43	160.2	53.1-54.2	63.0
RSVA8	7.58	159.9	133.8-134.4	87.0

Table 2: Docking results of *Electrophorus electricus*, *Mus musculus* and *Homo sapiens*.

Compound	<i>Electrophorus electricus</i>			<i>Mus musculus</i>			<i>Homo sapiens</i>	
	Energy ^a (pose)	cKi ^b	Interactions	Energy ^a (pose)	cKi ^b	Interactions	Energy ^a (pose)	cKi ^b
RSVA1	-22.2(1)	5.34E-08	W85/S202	-18.5 (1)	2.75E-05	S203/H447/Y341/W86	-16.8(1)	4.85E-05
RSVA2	-21.4(2)	2.06E-07	W85/S202	-18.0(2)	6.39E-05	S203/H447/Y341	-16.7(1)	5.74E-05
RSVA3	-19.2(2)	8.44E-06	W85/Y336/S202	-18.2(1)	4.56E-05	S203/Y341/W86	-14.1(2)	4.62E-05
RSVA4	-21.2(2)	2.89E-07	Y123/W281/S202	-18.8(1)	1.66E-05	S203/Y124/W86/Y341	-16.2(2)	1.33E-05
RSVA5	-21.7(2)	1.24E-07	Y123/Y336/W281/S202	-18.8(2)	1.66E-05	S203/W86/Y341	-16.1(1)	1.58E-05
RSVA6	-21.7(2)	1.24E-07	Y123/S202/W85	-19.3(2)	7.13E-06	S203/W86/H447/Y341	-15.2(2)	7.22E-06
RSVA7	-20.9(1)	4.79E-07	Y123/S202/H471/W85	-18.3(1)	3.85E-05	S203/Y124/Y341	-14.7(2)	1.68E-05
RSVA8	-15.2(6)	7.22E-03	Y123/S202/ H471/W85/Y336	-16.2(1)	1.33E-03	S203/H447/Y341	-15.5(1)	4.35E-03
Physostigmine	-14.5(5)	2.35E-02	Y336/S202/H471/W85	-9.3(2)	1.52E+02	Y124/W86/Y341/W286	-8.9(1)	2.99E+02
Resveratrol	-20.3(1)	1.32E-06	S202/H472/W85	-13(2)	2.96E-01	S203/W86/H447/Y341	-17.2(1)	2.47E-06
Acetylcholine	-13.3(5)	1.78E-01	S202/W85/H471	-12.6(1)	5.81E-01	S203/W86/Y341/Y124	-9.1(7)	2.14E+01

^a Best energy binding mode in kcal/mol. ^b Theoretical Ki in nM (cKi), according to PHOSRITHONG and UNGWITAYATORN, 2009.

Table 3: Main ADME results obtained with SwissADME (SA) and Molinspiration (MI) for compounds tested.

Compound	HB ^a donor	HB ^a acceptor	MW (g/mol) ^b		LogP		TPSA (Å ²) ^c	
	SA/MI	SA/MI	SA	MI	SA	MI	SA	MI
RSVA1	1	3	225.24	225.25	2.72	3.38	49.66	49.66
RSVA2	0	2	211.26	211.26	2.87	3.53	21.59	21.60
RSVA3	0	1	224.30	181.24	3.13	3.47	15.6	12.36
RSVA4	0	3/4	226.23	226.24	2.82	3.43	58.18	58.19
RSVA5	1	2	197.23	197.24	2.61	2.99	32.59	32.59
RSVA6	1	2	197.23	197.24	2.61	3.41	32.59	32.59
RSVA7	1	3	227.26	227.26	2.26	2.81	41.82	41.83
RSVA8	0	4	271.31	271.32	2.18	3.10	40.05	40.07
Resveratrol	3	3	228.24	228.25	2.26	2.99	60.69	60.68
Physostigmine	1	3/5	275.35	275.35	2.04	1.94	44.81	44.81

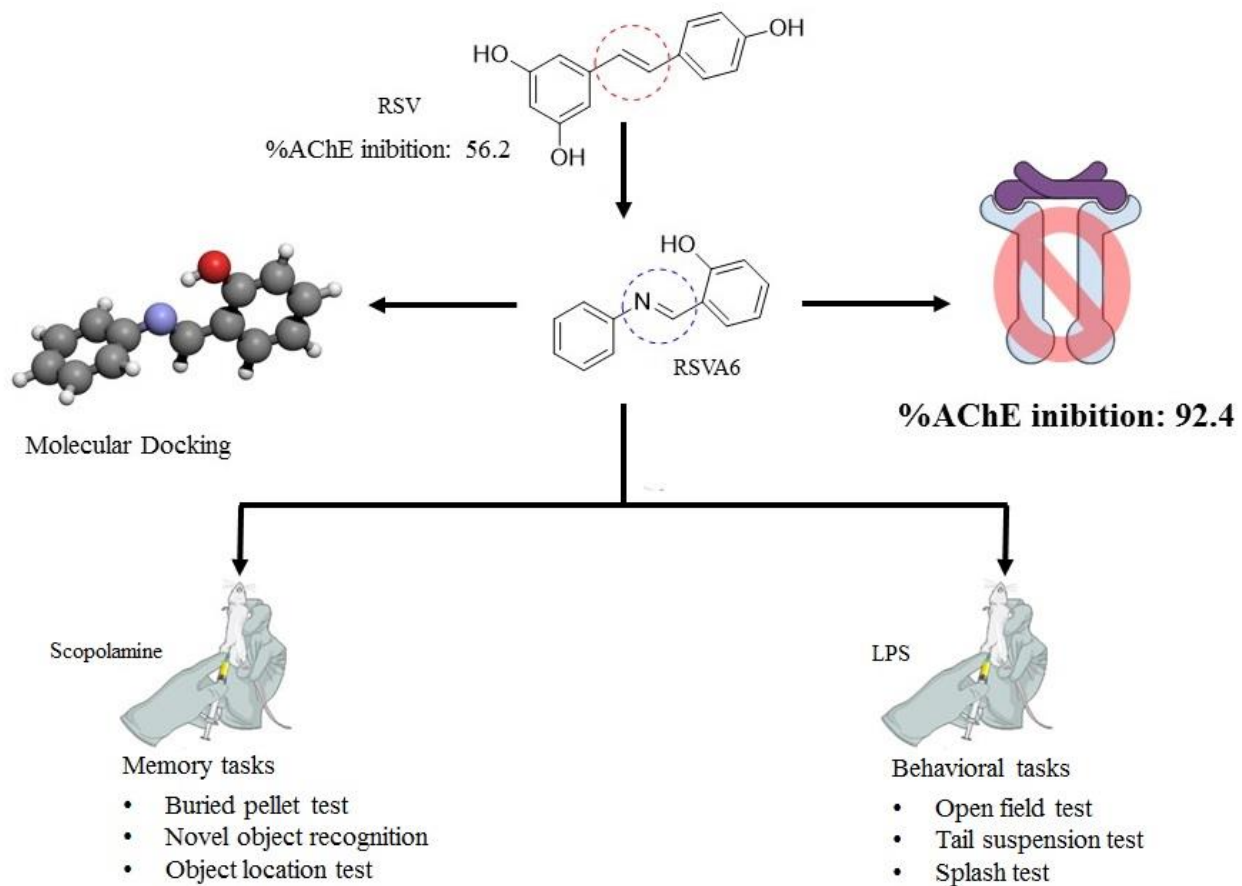
^aHB: Hydrogen Bond. ^bMW: molecular weight. ^cTPSA: total polar surface area.

Table 4: AChE inhibitory activity and IC₅₀ values of RSV and RSV analogues.

Compound	% AChE ^a inhibition	IC ₅₀ (M)
RSVA1	51.4	8.519 x 10 ⁻³
RSVA2	20.9	0.022
RSVA3	89.7	1.369 x 10 ⁻³
RSVA4	44.7	0.0102
RSVA5	20.7	0.023
RSVA6	92.4	2.225 x 10 ⁻³
RSVA7	44.8	9.126 x 10 ⁻³
RSVA8	40.2	0.011
Resveratrol	56.2	3.268 x 10 ⁻³
Physostigmine	100.0	7.692 x 10 ⁻⁶

Data represent the mean of percentage of two experiments. Physostigmine was used as reference drug. The best values are in bold. ^a Acetylcholinesterase of *E. electricus* (SIGMA, C2888).

Graphical Abstract



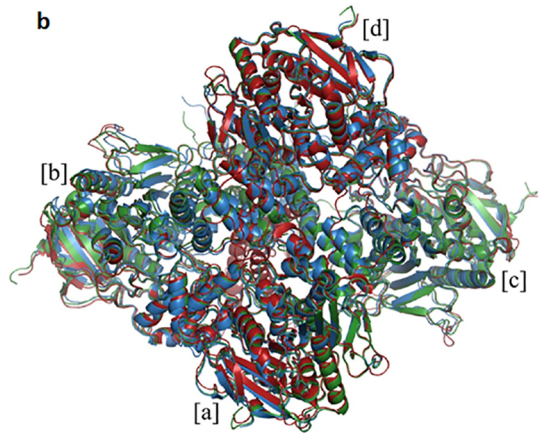
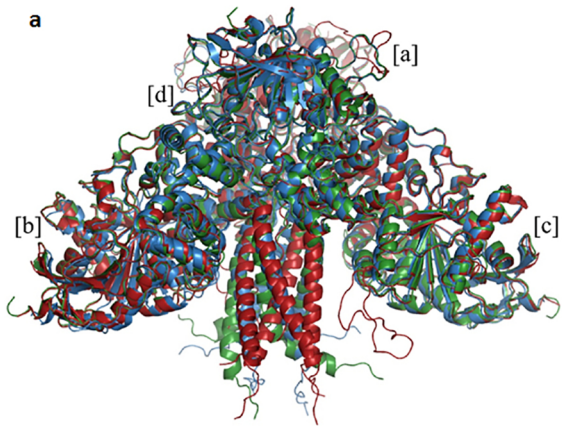


Figure 1

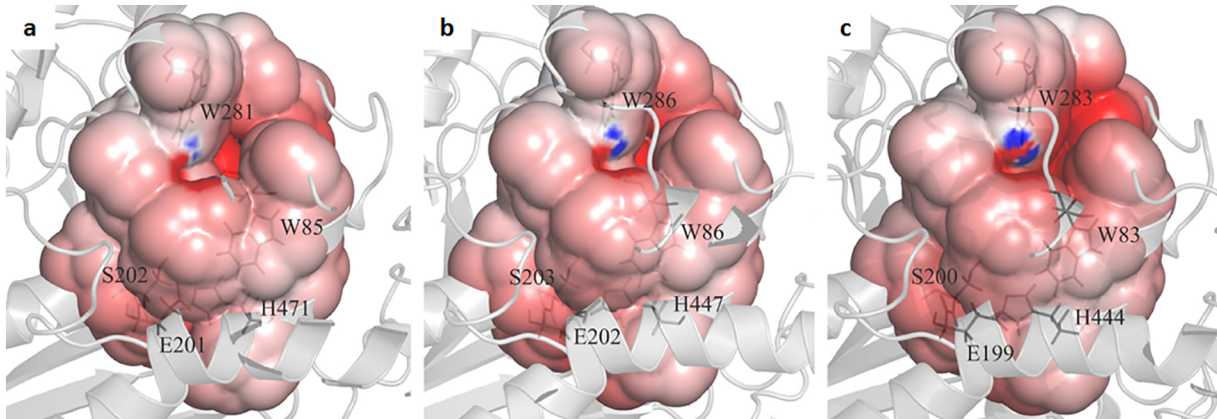


Figure 2

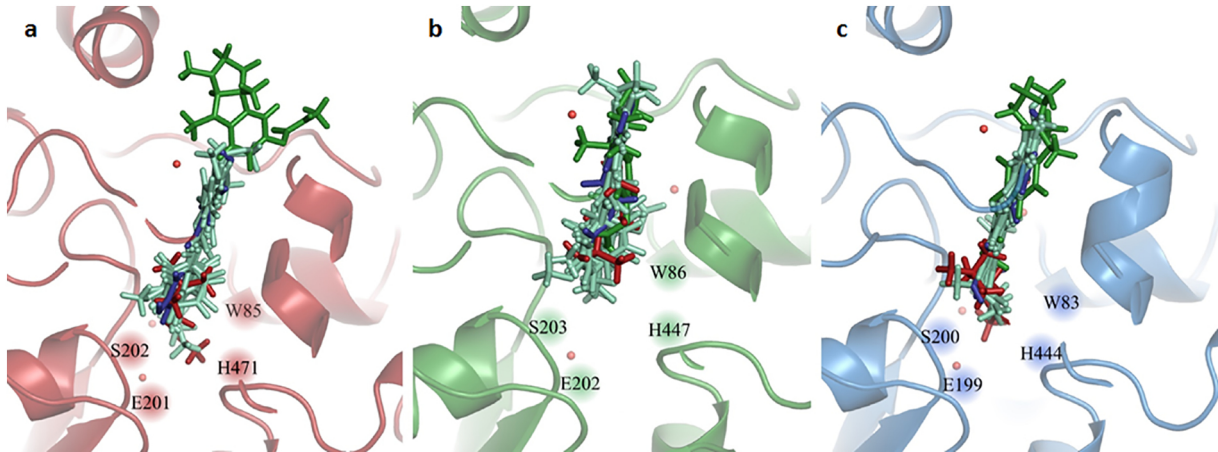


Figure 3

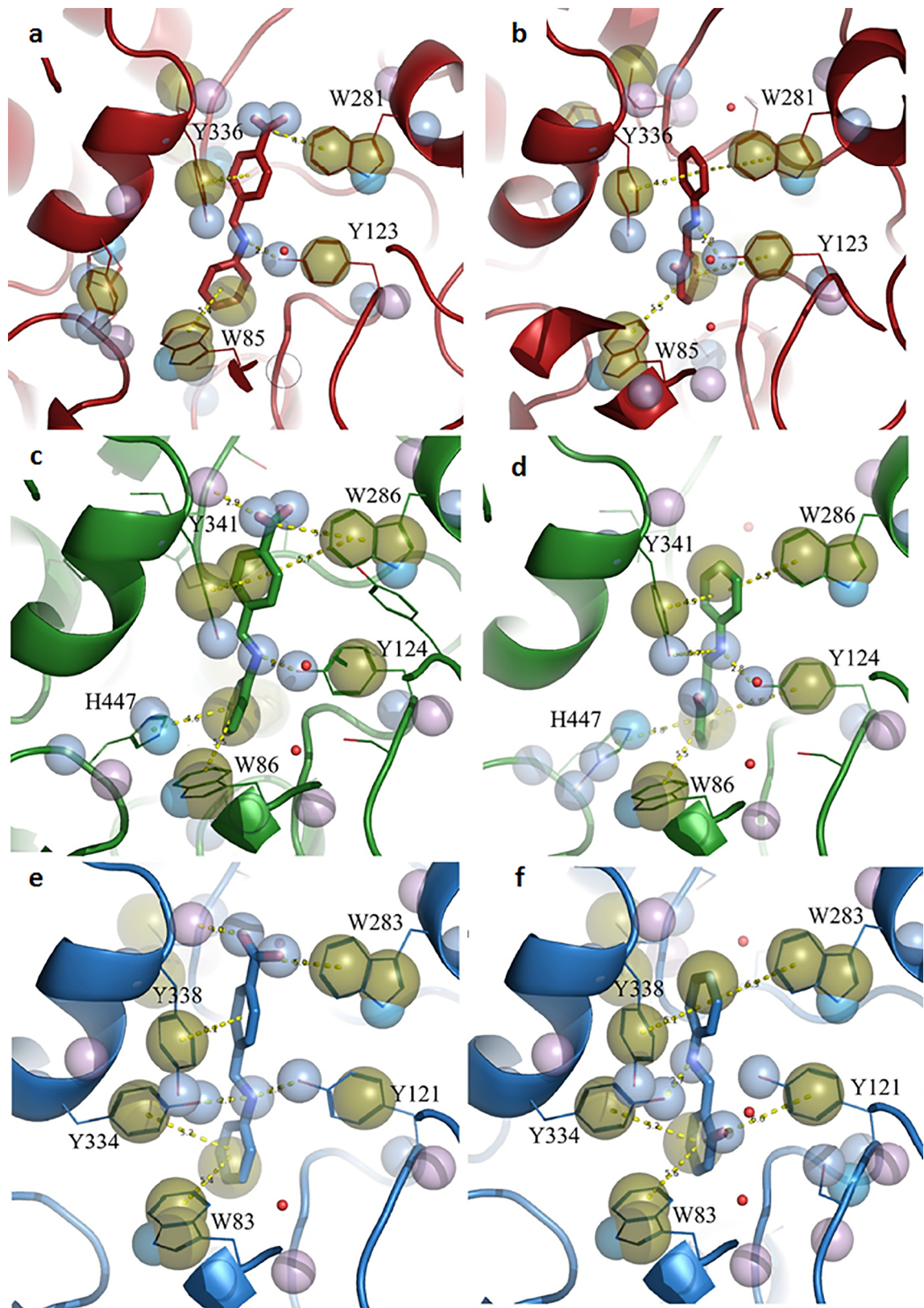


Figure 4

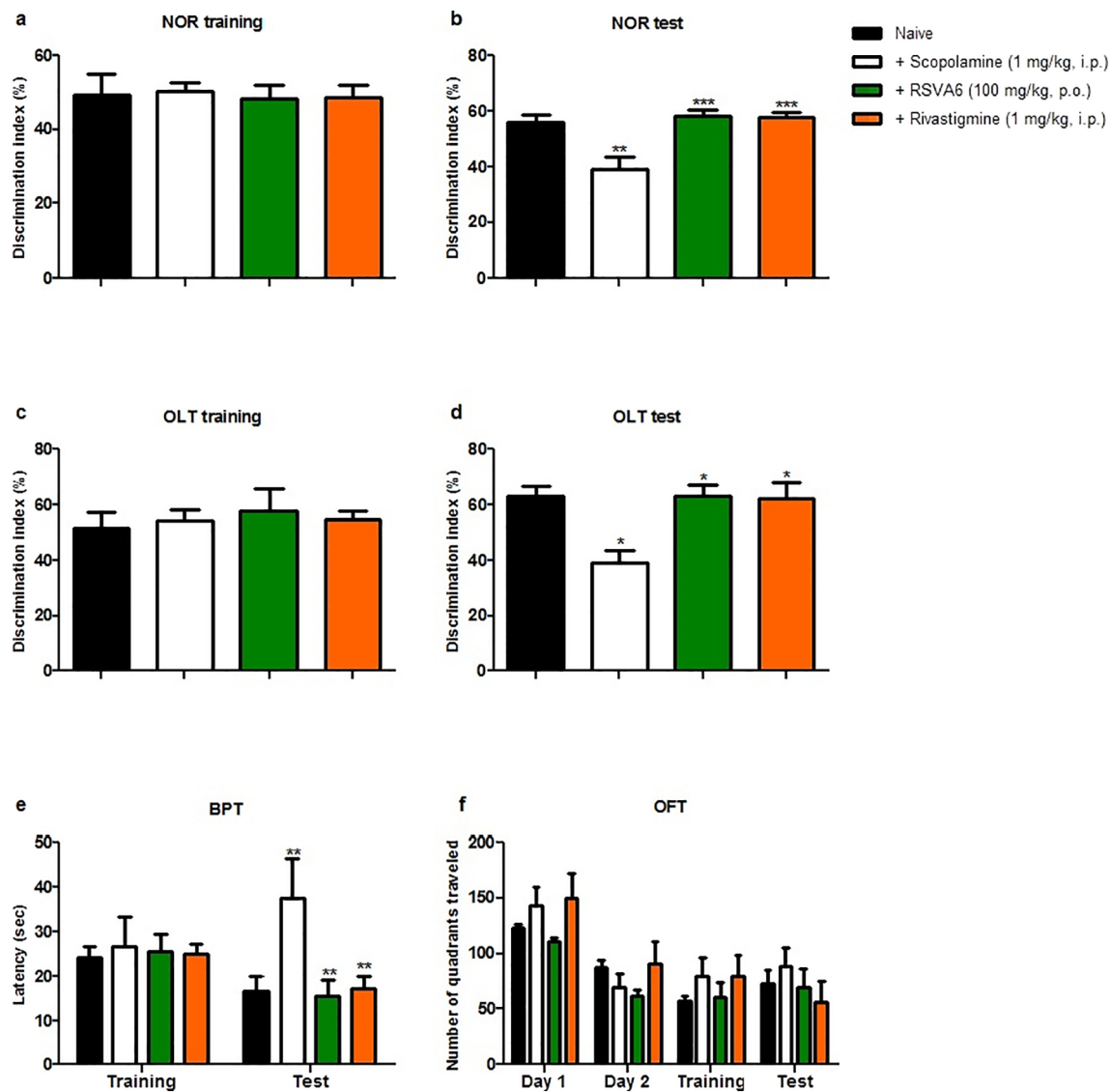


Figure 5

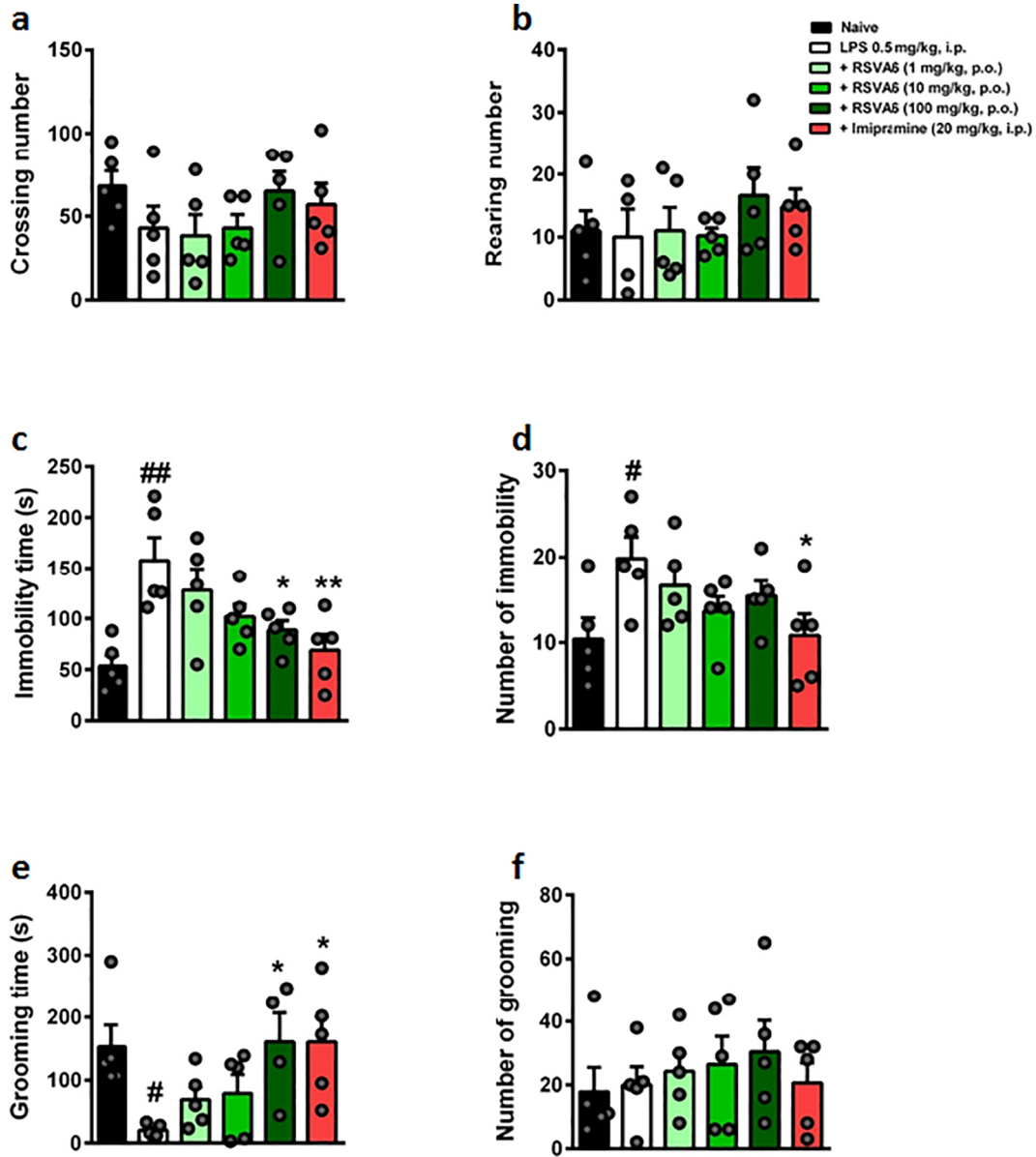


Figure 6

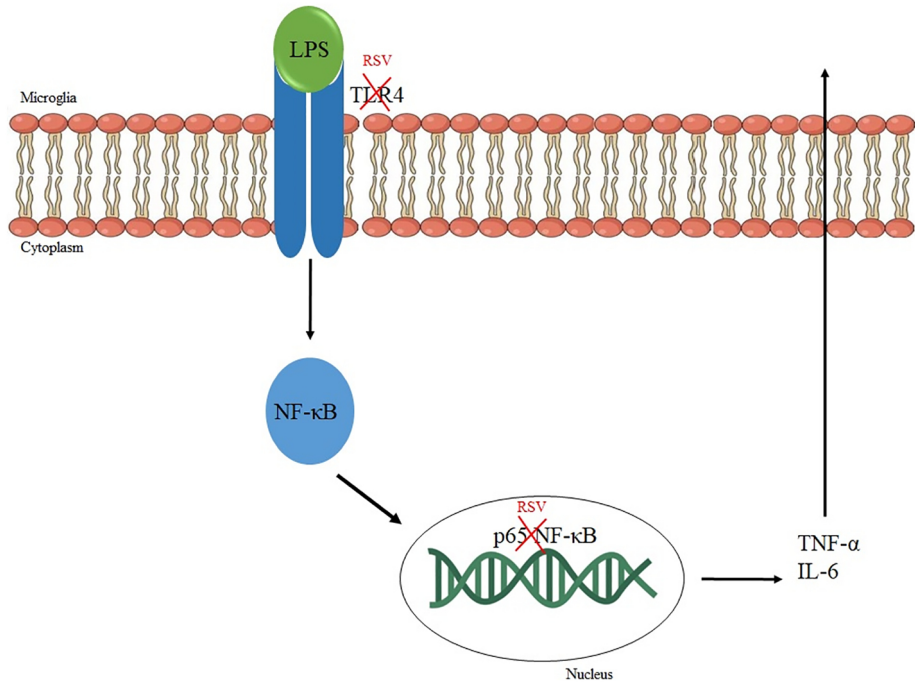


Figure 7